

LOAN DOCUMENT

PHOTOGRAPH THIS SHEET

①

DTIC ACCESSION NUMBER

LEVEL

INVENTORY

AFRL-ML-TY-TR-2002-4528

DOCUMENT IDENTIFICATION

19 Apr 2002

DISTRIBUTION STATEMENT A
Approved for Public Release
Distribution Unlimited

DISTRIBUTION STATEMENT

ACCESSION FOR	
NTIS	GRAM
DTIC	TRAC
UNANNOUNCED	
JUSTIFICATION	
BY	
DISTRIBUTION/	
AVAILABILITY CODES	
DISTRIBUTION	AVAILABILITY AND/OR SPECIAL
A-1	

DISTRIBUTION STAMP

DATE ACCESSIONED

DATE RETURNED

20020626 101

DATE RECEIVED IN DTIC

REGISTERED OR CERTIFIED NUMBER

PHOTOGRAPH THIS SHEET AND RETURN TO DTIC-FDAC

H
A
N
D
L
E

W
I
T
H

C
A
R
E

AFRL-ML-TY-TR-2002-4528



Numerical Models for Condenser and Evaporator Components of Fuel Cells

S.M. Ghiaasiaan, J.H. Yan, B.B. McCord

G.W. Woodruff School of Mechanical Engineering
Georgia Institute of Technology
Atlanta, GA 30332-0405

Approved For Public Release: Distribution Unlimited

**AIR FORCE RESEARCH LABORATORY
MATERIALS & MANUFACTURING DIRECTORATE
AIR EXPEDITIONARY FORCES TECHNOLOGIES DIVISION
139 BARNES DRIVE, STE 2
TYNDALL AFB FL 32403-5323**

AQ402-09-1989

NOTICES

USING GOVERNMENT DRAWINGS, SPECIFICATIONS, OR OTHER DATA INCLUDED IN THIS DOCUMENT FOR ANY PURPOSE OTHER THAN GOVERNMENT PROCUREMENT DOES NOT IN ANY WAY OBLIGATE THE US GOVERNMENT. THE FACT THAT THE GOVERNMENT FORMULATED OR SUPPLIED THE DRAWINGS, SPECIFICATIONS, OR OTHER DATA DOES NOT LICENSE THE HOLDER OR ANY OTHER PERSON OR CORPORATION; OR CONVEY ANY RIGHTS OR PERMISSION TO MANUFACTURE, USE, OR SELL ANY PATENTED INVENTION THAT MAY RELATE TO THEM.

THIS REPORT IS RELEASABLE TO THE NATIONAL TECHNICAL INFORMATION SERVICE
5285 PORT ROYAL RD.

SPRINGFIELD VA 22 161

TELEPHONE 703 487 4650; 703 4874639 (TDD for the hearing-impaired)

E-MAIL orders@ntis.fedworld.gov

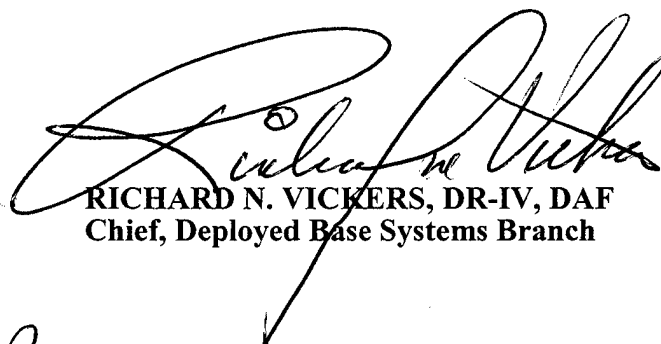
WWW <http://www.ntis.gov/index.html>

AT NTIS, IT WILL BE AVAILABLE TO THE GENERAL PUBLIC, INCLUDING FOREIGN NATIONS.


THIS TECHNICAL REPORT HAS BEEN REVIEWED AND IS APPROVED FOR PUBLICATION.



REZA SALAVANI, DR II, DAF
Program Manager



RICHARD N. VICKERS, DR-IV, DAF
Chief, Deployed Base Systems Branch



DONALD R. HUCKLE, JR., Colonel, USAF
Chief, Air Expeditionary Forces Technologies Division

Do not return copies of this report unless contractual obligations or notice on a specific document requires its return.

REPORT DOCUMENTATION PAGE			Form Approved OMB No. 0704-0188	
Public reporting burden for this collection of information is estimated to average 1 hour per response, including the time for reviewing instructions, searching existing data sources, gathering and maintaining the data needed, and completing and reviewing the collection of information. Send comments regarding this burden estimate or any other aspect of this collection of information, including suggestions for reducing this burden, to Washington Headquarters Services, Directorate for Information Operations and Reports, 1215 Jefferson Davis Highway, Suite 1204, Arlington, VA 22202-4302, and to the Office of Management and Budget, Paperwork Reduction Project (0704-0188), Washington, DC 20503.				
1. AGENCY USE ONLY (Leave blank)		2. REPORT DATE 19 April 2002		3. REPORT TYPE AND DATES COVERED Final Report 10 Nov 2000- Dec 2001
4. TITLE AND SUBTITLE Numerical Models for Condenser and Evaporator Components of Fuel Cells			5. CONTRACT NUMBERS F08637-00-C-7023	
6. AUTHOR(S) S. Mostafa Ghiaasiaan, PhD; J.H. Yan, PhD; B.B. McCord, PhD				
7. PERFORMING ORGANIZATION NAMES(S) AND ADDRESS(ES) Georgia Institute of Technology Office of Sponsored Programs Central Administration Atlanta, GA 30332-0420			8. PERFORMING ORGANIZATION REPORT NUMBER	
9. SPONSORING/MONITORING AGENCY NAME(S) AND ADDRESS(ES) AFRL/MLQD 139 Barnes Drive, Suite 2 Tyndall AFB FL 32403-5323			10. SPONSORING/MONITORING AGENCY REPORT NUMBER AFRL-ML-TY-TR-2002-4528	
11. SUPPLEMENTARY NOTES Availability of This Report Is Specified on Reverse of Front Cover.				
12a. DISTRIBUTION/AVAILABILITY STATEMENT Approved for public release, distribution unlimited			12b. DISTRIBUTION CODE A	
13. ABSTRACT (Maximum 200 words) This document reports on analytical models and computer programs that were developed for the design and analysis of evaporator and condenser components of modern fuel cells. Mechanistic models were developed for boiling and two-phase flow phenomena in Microchannel-based boilers. The modeled systems included straight Microchannel with known inlet/exit boundary conditions; helicoidally microchannels with known inlet/exit boundary conditions; straight, parallel microchannels connected to common inlet and exit plena; and straight, parallel microchannels connected to common inlet and exit manifolds. Models were also developed for fog formation/droplet growth resulting from the depressurization of a vapor-noncondensable mixture in an expander, and for droplet removal due to droplet-wall impaction when the aforementioned vapor-noncondensable-droplet mixture flows through a cyclone-type separator. Based on these models, computer programs suitable for design and analysis applications were developed.				
14. SUBJECT TERMS Condensation, Evaporation, Two-phase flow, Microchannel, Numerical models			15. NUMBER OF PAGES 101	
			16. PRICE CODE	
17. SECURITY CLASSIFICATION OF REPORT Unclassified	18. SECURITY CLASSIFICATION OF REPORT Unclassified	19. SECURITY CLASSIFICATION OF REPORT Unclassified	20. LIMITATION OF ABSTRACT UL	

Executive Summary

The objective of this project was to develop analytical models and computer programs for the design and analysis of evaporator and condenser components of modern fuel cells. Mechanistic models were developed for boiling and two-phase flow phenomena in Microchannel-based boilers. The modeled systems included straight Microchannel with known inlet/exit boundary conditions; helicoidally micro-channels with known inlet/exit boundary conditions; straight, parallel micro-channels connected to common inlet and exit plena; and straight, parallel micro-channels connected to common inlet and exit manifolds. Models were also developed for fog formation/droplet growth resulting from the depressurization of a vapor-non-condensable mixture in an expander, and for droplet removal due to droplet-wall impaction when the aforementioned vapor-non-condensable-droplet mixture flows through a cyclone-type separator. Based on these models, computer programs suitable for design and analysis applications were developed.

Table of Contents

Section	Page
Abstract	1
Table of Content	2
Notation	3
1.0 Introduction	6
2.0 Single-Channel Evaporator Models	8
2.1 General Remarks	8
2.2 Conservation Equations	10
2.2.1 Conservation Equations for Single-Phase Flow (Zones 1 and 4)	10
2.2.2 Conservation Equations for Boiling Two-Phase Flow (Zone 2)	11
2.2.3 Conservation Equations for the Film Evaporation Regime (Zone 3)	12
2.3 Flow Regime Maps and Interfacial Force Terms	14
2.3.1 Straight Channels	14
2.3.2 Helicoidal Channels	16
2.4 Wall Friction	17
2.5 Properties	19
2.6 Numerical Solution Method	20
3.0 Multi Channel Evaporator Models	21
3.1 General Remarks	21
3.2 Multi-Channel Evaporator with Inlet and Exit Plena	21
3.3 Multi-Channel Evaporator with Inlet and Exit Manifolds	22
3.3.1 Mathematical Model	22
3.3.2 Solution Method	26
4.0 Condenser and Moisture Separator Systems	36
4.1 General Remarks	36
4.2 Expander Models	36
4.2.1 Expander Types 1 and 4	37
4.2.2 Expander Types 2 and 3	41
4.2.3 Constitutive Relations	42
4.2.4 Solution Method	43
4.3 Cyclone-Type Separator	47
4.3.1 General Remarks	47
4.3.2 Cyclone Model	49
5.0 References	53
Appendix A: EVAPMC Code Manual	
Appendix B: DROPCON Code Manual	
Appendix C: CYCSEP Code Manual	

Notation

Major notation is listed below. Additional characters that have been used only once are defined where they are used.

A	Flow area
C_p	Specific heat
C_D	Drag coefficient
C_{vm}	Virtual mass term coefficient
D	Diameter
D_H	Hydraulic diameter
F	Force term
f	Friction factor
G	Mass flux
g	Gravitational constant
h	Specific enthalpy
h_{fg}	Latent heat of vaporization
h	Convection heat transfer coefficient
K	Pressure loss coefficient
k	Thermal conductivity; dimensionless constant
M	Molecular mass number
m	Mass fraction
\dot{m}	Mass flow rate
P	Pressure
P_i	Interfacial perimeter
q'	Thermal load, per unit length

q''	Heat flux
R	Universal gas constant
R_{cu}	Radius of curvature
Re	Reynolds number
S	Slip ratio
s	Specific entropy
T	Temperature
t	Time
U	Velocity
V	Volume
We_{cr}	Critical Weber number
\dot{W}	Power
X_{LM}	Lockhart-Martirelli parameter
x	Quality; mass fraction
Y	Mole fraction
z	Axial coordinate

Greek Letters

α	Void fraction
Γ	Evaporation mass rate, per unit volume
δ	Passage width
ϵ	Liquid volume fraction
σ_g	Geometric standard deviation

ϵ	Liquid volume fraction
η_r	Turbine isentropic efficiency
G	Angle of inclination with horizontal plane
ρ	Density

Subscripts

B	Bubble
e	Equilibrium
F	Frictional
f	Saturated liquids
G	Vapor-noncondensable
g	Saturated vapor
h	Homogeneous
i	Interphase
L	Liquid
LS	Liquid superficial
n	Noncondensable
s	Isentropic
TP	Two-phase
v	Vapor
1,2	Inlet, outlet

1. Introduction

Fuel cells are electrochemical systems that directly convert chemical energy from a stream of fossil fuel into electricity, by combining hydrogen and oxygen with the aid of a catalyst. Fuel cells do not apply the intermediate step of converting chemical energy into heat before producing electricity, and thus have lower irreversibility, have fewer moving parts, and do not generate many of the harmful combustion products typical of fossil fuel generators.

Fuel cells typically include an anode and a cathode, separated by an electrolyte. Several different types of electrolytes are used, including the proton exchange membrane, concentrated phosphoric acid, molten carbonate, and solid ceramic electrolyte.

In most fuel cells, a mixture of water vapor and hydrogen constitutes the anodic fluid, while the cathodic fluid is made of water vapor and oxygen (air). Although the cathodic fluid is often discarded, recycling of water content of the cathodic fluid may be necessary when the fuel cell is used in places where water is scarce. For recycling of the water content of the cathodic fluid, water should first be condensed in order to separate it from air. The condensate must then be evaporated before flowing into the anodic flow passages.

The design of the evaporator and condenser components of fuel cell systems, however, requires special care, due to their potentially unconventional configurations and working conditions. The evaporator may include small (micro) passages. The condenser, on the other hand, requires to be specially designed due to the very high concentrations of noncondensable (air) in the cathodic fluid.

The purpose of the effort reported in this document was to develop engineering analytical tools for the design, analysis, interpretation, and extrapolation of experimental data to be obtained during a number of novel evaporator and condenser systems. These included an

evaporator using a heated helicoidal microchannel; an evaporator using a large number of parallel microchannels connected at their two ends to common plenum; an evaporator using a large number of parallel microchannels connected at their two ends to common manifolds and condensation (due to spontaneous fog formation, or spray assisted), and droplet removal in a system consisting of an expander and a cyclone separator.

In what follows, the basic modeling features of a system consisting of a single heated microchannel evaporator are first briefly discussed in Chapter 2. The models dealing with multi-channel evaporators are then described in Chapter 3. In Chapter 4 the models developed for the condenser and moisture separation systems are described. Draft users manuals for several computer codes that have been completed in this project are then provided as Appendices.

Two other major tasks were also carried out in this project, which are not reported in this document, since they were not fully completed. These included the development of a surface condenser model based on the porous-media representation of the secondary side; and a generic one-dimensional model for the simultaneous fog formation/condensation on droplets and droplets removal due to droplet impaction on flow passage surfaces. The former task was undertaken early during the project, but was halted when a different condenser design was selected. The latter task was undertaken with the intention of developing a simple but flexible and general-purpose model for the simulation of condensation and droplet removal in flow passages with arbitrary geometry.

2.0 Single-Channel Evaporator Models

2.1 General Remarks

Two-phase flow and boiling in microchannels and small passages is of great interest and has been extensively studied recently (Ghiaasiaan and Abdel-Khalik, 2000). Micropassages and networks of microchannels can provide extremely large surface-to-volume ratios, and can thus dispose of extremely large volumetric thermal loads. Most of the applications involving cooling systems are based on subcooled forced convection and nucleate boiling, where large heat fluxes can be sustained with relatively low wall temperatures. For such applications the onset of nucleate boiling and onset of flow instability, and critical heat flux are important operational and safety thresholds. Other issues of interest include pressure drop, two-phase flow patterns and their characteristics, and void fraction. Only a brief review of issues relevant to narrow channels, which are of interest to this project, will be provided.

Investigations recently published, that deal with two-phase flow in micropassages include Ali and Kawaji (1991), Ale et al. (1993), Mishima et al. (1993), Wilmarth and Ishii (1994), and Fourar and Bories (1995). Depending on the liquid and gas (vapor) flow rates, several flow patterns may develop. For vertical channels, the void fraction can be obtained using the drift flux model (DFM), and Mishima et al. (1993) has proposed model constants applicable to thin passages.

An evidently important issue related to two-phase flow and boiling in thin passages is pressure drop. The aforementioned authors, with the exception of Wilmarth and Ishii (1994), all studied pressure drop as well. For laminar and turbulent single-phase flow, Jones (1974) has developed a simple and accurate method for the prediction of friction factors. A useful

correlation applicable to very narrow channels with rough surfaces has also been derived by John et al. (1988). Most of the authors who have measured two-phase pressure drop, have attempted to modify the constants in the correlation of Chisholm and Laird (1958). The resulting modifications, however, are often complicated and appear to be system-specific (Mishima et al., (1993). Recently, Ekberg (1999) measured pressure drops in horizontal thin annuli. A simple pressure drop correlation previously derived by Beattie and Whalley (1982) was subsequently found to well-predict the latter data. The correlation of Beattie and Whalley may thus be considered as an accurate and simple method for two-phase pressure drop calculation in thin micropassages.

Flow and heat transfer in helicoidal passages have been studied rather extensively in the past, since helicoidal channels are used in compact heat exchangers, chemical reactors, refrigeration and cryogenic systems. Recent studies of single-phase flow include Lin and Ebadian (1997) and Li, Lin and Ebadian (1998). Friction factor and heat transfer coefficient are both enhanced in comparison with straight channels. Most of the published studies deal with circular channels, however, and non-circular channels have received little attention (Shah and Joshi, 1987).

For two-phase flow, the coil orientation and helix angle are very important parameters. For vertically oriented helicoidal channels with small angle the flow regimes appear to have much in common with those observed in horizontal, straight channels (Kaji et al., 1984). Published studies dealing with two-phase flow regimes and pressure drop include Banerjee et al., (1969), Saxena et al. (1990), Awwad et al. (1994 a,b; 1995), Xin et al. (1990), Kang et al. (2000). Unfortunately, however, the past investigations were primarily concerned with circular

channels, and data and analysis dealing with two-phase flow in non-circular helicoidal flow passages are scarce.

2.2 Conservation Equations

One-dimensional conservation equations representing flow in a heated channel with uniform cross-section are presented in this section.

A schematic of a heated channel is displayed in Fig. 1. In general, the flow field can be divided into at least four zones; single-phase subcooled liquid near inlet (Zone 1); a single-phase superheated vapor near the exit (Zone 4); and boiling two-phase flow in-between. The boiling two-phase flow region is also divided into two different zones here for convenience. In Zone 3 all boiling regimes are considered. High quality (high void fraction) flow, representing the evaporation of an extremely thin liquid film in annular flow regime, however, is dealt with separately in Zone 4, since, for fast and efficient numerical solution, the two-phase flow conservation equations need to be presented slightly differently in the latter flow regime.

The following general assumptions are made:

1. The flow is one dimensional and steady-state
2. Channel cross-section is uniform
3. Where vapor and liquid are both present, thermal equilibrium between the two phases exists
4. Wall heat flux is known
5. The fluid is single-component

2.2.1 Conservation Equations for Single-Phase Flow (Zone 1 and 4)

Mass, momentum, and energy conservation equation are:

$$G = G_{in} \quad (1)$$

$$\frac{d}{dz} \left(\frac{G^2}{\rho_k} \right) = -\frac{dP}{dz} - \rho g \sin \theta - \frac{\tau_w P_f}{A} \quad (2)$$

$$\frac{d}{dz} (G h_k) = \frac{q'}{A} - g \sin \theta G \quad (3)$$

where $k = L$ for liquid (Zone 1 in Fig.1), and $k = v$ for vapor (Zone 4 in Fig. 1).

Equations (2,3) constitutes a set of ordinary differential equations with P and h_k as the state variables.

2.2.2 Conversation Equations for Boiling Two-Phase Flow (Zone 2)

The mixture mass and momentum conservation equations are:

$$\frac{d}{dz} [\rho_f U_f (1-\alpha) + \rho_g U_g \alpha] = 0 \quad (4)$$

$$\frac{d}{dz} [\rho_f (1-\alpha) U_f^2 + \rho_g \alpha U_g^2] = -\frac{dP}{dz} - [\rho_f (1-\alpha) + \rho_g \alpha] g \sin \theta - (-dP/dz)_F \quad (5)$$

The mixture energy equation is:

$$\frac{d}{dz} \left[\rho_f U_f (1-\alpha) \left(h_f + \frac{U_f^2}{2} + g z \sin \theta \right) + \rho_g U_g \alpha \left(h_g + \frac{U_g^2}{2} + g z \sin \theta \right) \right] = q' / A \quad (6)$$

The liquid -phase mass and momentum conservation equations are:

$$\frac{d}{dz} [\rho_f U_f (1-\alpha)] = -\Gamma \quad (7)$$

$$\begin{aligned}
\frac{d}{dz} \left[\rho_f (1-\alpha) U_f^2 \right] &= -(1-\alpha) \frac{dP}{dz} - \rho_f g (1-\alpha) \sin \theta \\
&+ F_i (U_g - U_f) - (1-\alpha) (-dP/dz)_F \\
&- \Gamma U_i + C_{VM} \left(U_g \frac{dU_g}{dz} - U_f \frac{dU_f}{dz} \right)
\end{aligned} \tag{8}$$

where Γ is the rate of mass evaporation per unit length of the channel. Elimination of Γ between the above two equations gives:

$$\begin{aligned}
\frac{d}{dz} \left[\rho_f (1-\alpha) U_f^2 \right] &= -(1-\alpha) \frac{dP}{dz} - \rho_f g (1-\alpha) \sin \theta \\
&+ F_i (U_g - U_f) - (1-\alpha) (-dP/dz)_F \\
&+ U_i \frac{d}{dz} \left[\rho_f U_f (1-\alpha) \right] + C_{VM} \left(U_g \frac{dU_g}{dz} - U_f \frac{dU_f}{dz} \right)
\end{aligned} \tag{9}$$

Equations (4), (5), (6), and (9) are four coupled ordinary differential equation with P , U_f , U_g and α as their state variables.

2.2.3 Conservation Equation for the Film Evaporation Regime (Zone 3)

Although the conservation equations of previous section are directly appreciable here, the numerical solution of the equations is somewhat problematic in this regime. The difficulty is due to the fact that in this regime $\alpha \approx 1$ and $\frac{d\alpha}{dz} \approx 0$, and these render the set of ordinary differential equations (ODEs) stiff. Furthermore, since the two-phase equations must in principle be integrated until $x=1$ and $\alpha=1.0$ (i.e., complete evaporation of the annular film), the set of ODEs becomes stiffer as the integration proceeds. The liquid-phase momentum equation (Eqn.

9) is the main source of difficulty since it represents the acceleration of a fluid with essentially zero inertia.

To avoid this difficulty, the two-fluid scheme of the previous section is simplified by dropping Eqn. (9), (i.e. the liquid phasic momentum equation). Instead, the following slip ratio expression of Zivi (1968) is used:

$$S = U_g / U_f = (\rho_f / \rho_g)^{1/3} \quad (9-a)$$

The above expression has been derived based on the assumption of minimum entropy generation in annular flow.

Using Eqn. (9a), U_g is eliminated from Eqn. (4-6), leading to three ODEs, with P , U_f and α as the state variables. The void fraction, furthermore, is eliminated in favor of (equilibrium) quality, x_e . The resulting equations, which are given below, can be integrated without difficulty.

$$\frac{1}{x_e} \frac{dx_e}{dz} = \frac{1}{\rho_g} \left(\frac{\partial \rho_g}{\partial P} \right)_{sat} \frac{dP}{dz} + \frac{1}{U_g} \frac{dU_g}{dz} \quad (10-a)$$

$$\begin{aligned} G \frac{d}{dz} (x_e U_g) &= -\alpha \frac{dP}{dz} - \rho_g \alpha g \sin \theta \\ -F_i (U_g - U_f) &- \alpha (-dP/dz)_F \\ + G U_i \frac{dx_e}{dz} \end{aligned} \quad (10-b)$$

$$G \frac{d}{dz} \left[(1-x_e) \left(h_f + \frac{U_f^2}{2} \right) \right] + G \frac{d}{dz} \left[x_e \left(h_g + \frac{U_g^2}{2} \right) \right] = q' / A \quad (10-c)$$

It should be noted that, deriving Eqn. (10-a), $\frac{d\alpha}{dz} \approx 0$ has been assumed.

2.3 Flow Regime Maps and Interfacial Force Terms

2.3.1 Straight Channels

Two-phase flow regimes in narrow, rectangular channels are complicated, since velocity slip readily occurs in such channels. A good review can be found in Ghiaasiaan and Abdel-Khalik (2001).

A good representative of previously published studies is that of Ali and Kawaji (1991). The observed regimes in their channels generally include bubbly (small bubbles); intermittent, and annular. The intermittent regime includes slug, and churn flow patterns. Rivulet flow can also occur at very low liquid superficial velocities. Complicated flow patterns were also reported by Fourar and Bories (1995). Published relevant data have significant disagreement, and no reliable flow regime map is currently available (Ghiaasiaan and Abdel-Khalik, 2001). Therefore, in this study, a simple but well-tested flow regime transition model will be used. This simple method has been successfully used in the past for two-phase flow in channels undergoing rapid evaporation. (Ghiaasiaan and Geng, 1997). Accordingly, we assume:

$$\text{Bubbly for } \alpha \leq 0.2 \quad (11)$$

$$\text{Annular for } \alpha \geq 0.80 \quad (12)$$

$$\text{Intermittent for } 0.2 \leq \alpha \leq 0.75 \quad (13)$$

In bubbly regime, we assume bubbles with diameters:

$$D_B = \min \left[\frac{\sigma}{\rho_L (U_G - U_L)^2} We_{cr}, \frac{\delta}{2} \right] \quad (14)$$

where δ = width of the channel, and

$$We_{cr} = 3. \quad (15)$$

Equation (14) assumes that aerodynamic dispersion is responsible for bubble breakup. The void fraction and number density of bubbles in bubbly flow regime are related according to

$$N = \frac{\alpha}{\frac{\pi}{\sigma} D_B^3} \quad (16)$$

Furthermore, the interfacial area concentration can be found from:

$$\frac{P_i}{A} = N \pi D_B^2 \quad (17)$$

The interfacial force per unit mixture volume can now be found from:

$$F_i = \frac{3}{4} \alpha \frac{C_D}{D_B} \rho_f |U_g - U_f| \quad (18)$$

where:

$$C_D = \frac{24}{\text{Re}_B} (1 + 0.15 \text{Re}_B^{0.687}) \quad (19)$$

$$\text{Re}_B = \rho_f |U_g - U_f| D_B / \mu_f \quad (20)$$

In the annular flow regime, it can be shown that

$$F_i = \frac{P_i}{A} C_{fi} \frac{1}{2} |U_g - U_f| \quad (21)$$

where it is assumed that

$$C_{fi} = 0.05 \quad (22)$$

In the intermittent regime (see Eqn. (13)), F_i is found by interpolation between the bubbly and annular regime values at $\alpha = 0.25$ and $\alpha = 0.8$, respectively, using the void fraction as the interpolation parameter.

The virtual mass force term, the last term on the right side of Eqns. (8) or (9), involves the constant C_{VM} . This coefficient is represented as:

$$C_{VM} = \alpha(1-\alpha)[\rho_f(1-\alpha) + \rho_g\alpha] \quad (23)$$

2.3.2 Helicoidal Channels

The above models, strictly speaking, are appreciable to straight channels and may need to be modified before they can be applied to helicoidal channels. Little is known about the flow regimes in helicoidal channels that have rectangular cross-sections, however. A brief discussion follows.

For vertically-oriented helicoidals, when the helix angle is very small, and provided that $D_H / R_{cu} \ll 1$ (where R_{cu} represents the coil radius of curvature), the flow regimes can be expected to be similar to those occurring in straight channels, and commonly-applied methods for two-phase flow pressure drop can also be used (Banerjee et al., 1969). Kaji et al. (1984) also noted similarity between straight, horizontal channels and vertical helicoidal channels with small helix angles, with respect to flow regimes. A good experimental study aimed at the measurement and correlation of two-phase friction factors in vertical helicoidal channels with circular cross-section with helix angles in the $0.5^\circ \square 10^\circ$, has been reported by Xin et al. (1996). The developed empirical correlation for friction factor in the latter study of course may not be directly applicable to noncircular channels.

Awwad et al. (1995) measured and correlated the air-water two-phase pressure drop in a horizontally-oriented helicoidal tube, for helix angles in the $1.0\text{-}20^\circ$ range, and pipe diameters in the 330 – 670mm range. The single-phase friction factors in their experiments agreed well with

the correlations of Manlapaz and Churchill (1980) for laminar flow, and Ito (1959) for turbulent flow. They correlated their two-phase flow pressure drop data as:

$$\phi_L = \left[1 + \frac{X_{LM}}{CF_d^n} \right] \left(1 + \frac{12}{X_{LM}} + \frac{1}{X_{LM}^2} \right)^{1/2} \quad (24)$$

where X_{LM} is the Martinelli factor, and $n = 0.576$, and $C = 7.79$ for $F_d < 0.3$; while $n = 1.3$ and $C = 13.56$ otherwise. The dimensionless number F_d is defined as:

$$F_d = \frac{U_{LS}^2}{gD} (D/2R_{cu})^{0.1} \quad (25)$$

where U_{LS} is the liquid-phase superficial velocity and D is the (circular) channel diameter.

For horizontal helicoidal channels, due to the apparent lack of better and more relevant data and correlations, Eqn. (24) can be used for rectangular channels, with D replaced with D_u , albeit that the correlation has been developed originally for circular channels. Should horizontally-oriented helicoidal channels be of interest, furthermore, the flow regime model and the interfacial force terms described in the previous section will be unlikely to be accurate, and may need modification.

For the vertical helicoidal configuration, the methodology described in the previous section is applicable when the helix angle is very small, and for circular cross-section channels. Major modifications may be needed otherwise, however.

2.4 Wall Friction

Since rectangular channels are of interest, only models relevant to this geometry are used at this time. For single-phase flow, and assuming a straight channel, laminar-to-turbulent flow regime transition is assumed to occur when $Re > 2,300$, where the Reynolds number is defined

based on the hydraulic diameter. For laminar flow, the correlation of Shah and London (1987) (See Kakac et al., 1987) is used, whereby the D'Arcy friction factor f is obtained from:

$$f Re = (24) \left[1 - 1.3553 \alpha^* + 1.9467 \alpha^{*2} - 1.7012 \alpha^{*3} + 0.9564 \alpha^{*4} - 0.2537 \alpha^{*5} \right] \quad (26)$$

where α^* is the ratio between smaller and larger sides of the rectangular cross-section. For turbulent flow, the correlation of Shah and Bhatti (1987), (Kakac et al., 1987) is used, where by:

$$F = (1.0875 - 0.1125 \alpha^*) f_c \quad (27)$$

where f_c is the circular-channel correlation of Techo et al (Kakac et al., 1987):

$$\frac{1}{\sqrt{f_c}} = 1.7372 \ln \left[\frac{Re}{1.964 \ln Re - 3.8215} \right] \quad (28)$$

The above correlations is supposed to be valid in the $5000 \leq Re \leq 10^7$. Although Bhatti and shah tested Eqn. (27) within the above range, we will use the correlation for $Re > 2300$ for simplicity. For two-phase flow the empirical correlation of Beattie and Whalley (1982) is used. Define two-phase Reynolds number as:

$$Re_{TP} = \frac{GD_H}{\mu_{TP}} \quad (29)$$

where

$$\rho_h = \alpha \rho_g + (1 - \alpha) \rho_f \quad (30)$$

$$\mu_{TP} = \alpha_h \mu_g + (1 - \alpha_h) (1 + 2.5 \alpha_h) \mu_f \quad (31)$$

$$\alpha_h = \frac{y / \rho_g}{y / \rho_g + \frac{1 - y}{\rho_f}} \quad (32)$$

$$y = \frac{\rho_g U_g \alpha}{\rho_g U_g \alpha + \rho_f U_f (1 - \alpha)} \quad (33)$$

The two-phase Reynolds number defined in Eqn.(28) is now used in single-phase friction factor correlations in order to derive the two-phase flow friction factor, f_{TP} . The frictional pressure gradient in the channel is then obtained from:

$$\left(-dP/dz\right)_F = f_{TP} \frac{G^2}{2\rho_h} \quad (34)$$

It should be mentioned that the correlation of Beatttie and Whalley is based on circular channel data, and uses the well-known Colebrook-White correlation for turbulent single-phase friction factor.

It should also be emphasized that the above methods may need to be modified for application to helicoidal channels.

2.5 Propertties

Thermodynamic and transport properties of subcooled and saturated water, and saturated and superheated steam, are calculated using the routine WSPROP, previously developed and used by author and co-workers (Ghiaasiaan et al., 1995). WSPROP contains several explicit approximating expressions for calculating liquid water and steam thermodynamic properties borrowed from Kuck (1982). The partial derivatives of water and steam thermodynamic properties are also calculated in WSPROP by differentiating the relevant explicit approximating expressions (Kuck, 1982). Water and steam thermal conductivity and viscosity are obtained by interpolation on relevant property tables of Grigull et al., (1984). The interpolation algorithms are based on Press et al. (1988).

2.6 Numerical Solution Method

The conservation equations were expanded using appropriate thermodynamic relations and cast in the form of coupled sets of ordinary differential equations (ODEs), using the methodology described elsewhere (Ghiaasiaan and Geng, 1997; Ghiaasiaan et al., 1995). The details can be found in the latter references and will not be repeated here. The resulting sets of ODEs have the following generic form:

$$A \frac{dY}{dz} = C \quad (35)$$

when Y is a column vector with N elements the state variables, with N representing the number of equation, and A is an $N \times N$ coefficient matrix. The column vector C is an N -element vector.

For subcooled single-phase liquid or (superheated) vapor flow, given the fact that $G = \text{const}$, (see Eqns. (1-3),

$$Y = (h_k, P)^T \quad (36)$$

with $k = L$ and v for liquid and vapor respectively. For the two-phase flow region.

$$Y = (P, U_g, U_f, \alpha)^T \quad (37)$$

Finally, for the film evaporation regime:

$$Y = (P, U_g, x_e)^T \quad (38)$$

where x_e is the local equilibrium quality.

The above sets of ODEs are numerically integrated, in tandem, using the DVODE equation solver package which is similar to the equation solves described by Hindmarsh (1980). This numerical package uses a robust and efficient variable-step and variable-order numerical method that is particularly useful for the solution of stiff equation systems.

3.0 Multi-Channel Evaporator Models

3.1 General Remarks

Multi-channel evaporators, consisting of a large number of parallel and geometrically-identical straight heated channels connected to two common plena or manifolds at their two ends, have been considered as possible designs for the fuel cells of interest. The models briefly described below have been developed for such multi-channel evaporator systems.

It should be noted that the multi-channel models described here utilize the single-channel models described in chapter 2 of this report for analyzing the flow and heat transfer phenomena in each individual channel. The crucial calculations in the multi-channel model deal with the correct implementation of the inlet and exit channel boundary conditions, and this can only be done by carefully-designed iterative schemes.

3.2 Multi-Channel Evaporator with Inlet and Exit Plena

The modeling of this type of multi-channel evaporators is actually relatively simple, although the iterative solution procedures needed for this purpose are computationally expensive. The simplicity results from the fact that the parallel channels all have common inlet and exit pressures.

The following assumptions are made:

1. The parallel channels have the same length and thermal loads.
2. The channels can be divided into a finite number of groups. In each group, the channels are geometrically identical.
3. Inlet pressure and fluid conditions are the same for all channels.

4. The channels all open to the same plenum, and therefore have the same exit pressure.

Accordingly, an algorithm was developed that can be used to distribute a known, total mass flow rate among a given set of parallel channels. The algorithm, briefly, is as follows.

The average mass flux in the channels is first calculated. Using this mass flux as the first guess, the conservation equations described in Chapter 2 are solved for a channel from each channel group, leading to the calculation of channel exit pressures. The pressure drops of all channel groups are thus obtained and are averaged. The pressure drop in each group is then compared with the aforementioned average pressure drop. The mass flux for each tube group is then re-adjusted by multiplying it by the ratio of channel exit pressure calculated in the previous iteration and the average exit pressure of all channels. The entire procedure is then repeated. Convergence is obtained when the differences among the calculated exit channel pressures are all within a specified tolerance value.

The computer program that performs this type of calculations (EVAP10D) has been successfully tested for an imaginary system consisting of three groups of tubes, each group consisting of five geometrically-identical channels.

However, the algorithm at its present form converges relatively slowly, and the aforementioned computer program is consequently computationally expensive.

3.3 Multi-Channel Evaporator with Inlet and Exit Manifolds

3.3.1 Mathematical Model

The system to be modeled is depicted in Figure 2. The geometry clearly shows that the inlet and exit conditions for the individual channels will be different, and the distribution of the

fluid mass among the channels will be non-uniform. Once again, a method must be devised to iteratively distribute the mass among the channels such that all boundary and interface conditions are correctly satisfied.

The following assumptions are made.

1. The flow in all channels, and along both manifolds, is one-dimensional and steady-state.
2. The fluid at the exit of all the channels is pure saturated or superheated vapor.
3. At inlet to the inlet plenum, the fluid is subcooled liquid.
4. For pressure drop calculation purposes, the vapor throughout the exit plenum can be assumed to be pure saturated vapor.
5. The channels are geometrically identical.
6. The thermal load of all the channels are the same.

In what follows, the fluid momentum equations are first derived using the vector momentum method. The algorithm used for the iterative solution of the equation is then briefly described.

We will start with the control volume depicted in Fig. 3, which represents the segment of the inlet manifold between the manifold's inlet, and the inlet to the first heated channel. Assume that the static pressure at inlet to the inlet plenum is P_{in}^* . This pressure evidently depends on the details of the flow field upstream from the inlet plenum, and is assumed known.

Applying the momentum conservation principle, in the direction of the inlet manifold, to the depicted control volume, one gets:

$$P_{in}^* - P_{m,in,1} + \left(\frac{\dot{m}_{tot}^2}{\rho_L A_{m,in}^2} - \frac{\dot{m}_{m,in,1}^2}{\rho_L A_{m,in}^2} \right) - \frac{f_1 Z_o \rho_L}{2 A_{m,in} D_{h,m,in}} \left(\frac{\dot{m}_{tot}}{\rho_L A_{m,in}} \right)^2 - K_{ent} \frac{1}{2 \rho_L} \left(\frac{\dot{m}_{tot}}{A_{m,in}} \right)^2 = 0 \quad (39)$$

Furthermore:

$$P_{m,in,1} - P_{in,1} = K_{T,ent} \frac{\dot{m}_1^2}{2 \rho_L A_1^2} \quad (40)$$

$$\dot{m}_{m,in,1} = \dot{m}_{tot} - \dot{m}_1 \quad (41)$$

The parameters in the above equations have the following definitions:

- $A_{m,in,1}$ = Inlet manifold cross-sectional area
- A_1 = Channel #1 cross-sectional area
- $D_{h,m,in}$ = Inlet manifold hydraulic diameter
- K_{ent} = Manifold entrance pressure loss coefficient
- $K_{T,ent}$ = Pressure loss coefficient due to entrance in a T-junction
- f_i = D'Arcy friction factor for the inlet manifold

Other parameters, including pressures and mass flow rates are defined in Fig. 3.

Now, consider the control volume depicted in Fig. 4, which represents the segment of the inlet manifold between channels $j-1$ and j . For this control volume one can write

$$P_{m,in,j-1} - P_{m,in,j} + \left(\frac{\dot{m}_{m,in,j-1}^2}{\rho_L A_{m,in}^2} - \frac{\dot{m}_{m,in,j}^2}{\rho_L A_{m,in}^2} \right) - \frac{f_j S \rho_L}{2 A_{m,in} D_{h,m,in}} \left(\dot{m}_{m,in,j-1} / \rho_L A_{m,in} \right)^2 = 0 \quad (42)$$

$$P_{m,in,j} - P_{in,j} - K_{T,ent} \frac{\dot{m}_j^2}{2\rho_L A_j^2} = 0 \quad (43)$$

$$\dot{m}_{m,in,j} = \dot{m}_{m,in,j-1} - \dot{m}_j \quad (44)$$

The definitions of parameters in the above equation are:

\dot{m}_j = Mass flow rate in the j th channel

A_j = Area of the j th channel

f_j = Friction factor in the depicted segment of the manifold

S = The spacing between two adjusted channels

Flow rates and pressures are defined in Fig. 4. Figure 4, and Eqns.(40-42) in fact apply to channels 2 through N , with N representing the total number of channels.

Similar equation sets can be set up for the exit manifold. Figure 5 depicts the control volume at the exit of the exit manifold. For this control volume one can write:

$$\begin{aligned} P_{m,o,1} - P_{out}^* + \left(\frac{\dot{m}_{m,o,1}^2}{\rho_g A_{m,o}^2} - \frac{\dot{m}_{tot}^2}{\rho_g A_{m,o}^2} \right) \\ - \frac{f_1 Z_o \rho_g}{2 A_{m,o} D_{h,m,o}} \left(\frac{\dot{m}_{tot}}{\rho_g A_{m,o}} \right)^2 \\ - K_{exit} \frac{1}{2 \rho_g} \frac{\dot{m}_{tot}^2}{A_{m,o}^2} = 0 \end{aligned} \quad (45)$$

$$P_{m,o,1} - P_{out,1} + K_{T,exit} \frac{\dot{m}_1^2}{2 \rho_g A_1^2} = 0 \quad (46)$$

where:

K_{exit} = Manifold exit loss coefficient

$K_{T,exit}$ = Loss coefficient for exit T junction

$A_{m,o}$ = Area of the exit manifold

$D_{h,m,o}$ = Hydraulic diameter of the exit manifold

Likewise, for the control volume depicted in Fig. 6, we can write:

$$P_{m,o,j} - P_{m,o,j-1} + \left(\frac{\dot{m}_{m,o,j}^2}{\rho_g A_{m,o}^2} - \frac{\dot{m}_{m,o,j-1}^2}{\rho_g A_{m,o}^2} \right) \quad (47)$$

$$- \frac{f_i S \rho_g}{2 A_{m,o} D_{h,m,o}} \left[\left(\frac{\dot{m}_{m,o,j-1}}{\rho_g A_{m,o}} \right)^2 \right] = 0$$

$$\dot{m}_{m,o,j-1} = \dot{m}_{m,o,j} + \dot{m}_j \quad (48)$$

$$P_{m,o,j} = P_{out,j} - K_{T,exit} \frac{1}{2} \frac{\dot{m}_j^2}{\rho_g A_j^2} \quad (49)$$

3.3.2 Solution Method

The equations presented in the previous section, when written for all the control volumes in the inlet and exit manifolds, form a set of algebraic equations which would be closed for the conditions to be described shortly, where the single-channel models described in Chapter 2 are included. In other words, with geometric characteristics of a particular channel as well as its thermal load and inlet fluid enthalpy all fixed, the entire single-channel model can be thought of as a highly non-linear algebraic equation in the generic form:

$$f(P_{in,j}, P_{out,j}, \dot{m}_j) = 0 \quad (50)$$

The above equations, including those represented by Eqn.(49) for $j = 1, 2, \dots, N$, constitute a closed set of equations, with unknown that include: $\dot{m}_j, P_{m,in,j}, P_{m,o,j}, P_{in,j}, P_{out,j}$, etc.. Furthermore, two of the following three quantities must be known: P_{in}^*, P_{out} , and \dot{m}_{tot} .

An iterative solution of there equation is evidently difficult and time consuming. After trying a number of different methods, the following novel method was eventually found to be the most efficient.

We consider the conditions where P_{in}^* and \dot{m}_{tot} are assumed known. The following procedure is then used. (Note that , if P_{in}^* or \dot{m}_{tot} is the unknown the method is still valid, only more iteration, for example on P_{in}^* when it is an unknown are needed).

1. Knowing the total mass flow rate and inlet/exit pressures for the manifolds, the single-channel

model is applied to generate a table with about 60 entries, providing predicted values of channel exit pressure given inlet channel pressure and channel mass flow rate. These runs are not iterative and can be performed with relatively little computation. The entries in this table, when used along with an interpolation routine, in fact represent the numerical solution for Eqn. (49).

2. The conservation equation for the first channel, and the segments of the inlet and exit manifolds that are located between the first channel and their entrance and exit, respectively, are iteratively solved. These equations includes Eqn. (38-40), (44,45), and (49) with $j = 1$. (Note that the latter equation is replaced by an interpolation routine that interpolates in the afore-mentioned table). The equation set is in fact closed, and would lead to the calculation of $\dot{m}_1, P_{out}^*, \dot{m}_{m,in,1}, P_{m,in,1}, \dot{m}_{m,o,1}, P_{m,o,1}$.

3. The solution in step 2 above provides the boundary conditions for the system consisting of the channel #2, and the segments of the inlet and exit manifolds that are located between the first and second channels. The relevant equations included Eqns. (41-43),

and (46-48), and (49), and their iterative solution leads to the calculation of \dot{m}_2 ,

$$P_{m,in,1}, \dot{m}_{m,in,j}, P_{m,o,j}, \dot{m}_{m,o,j}, P_{in,j}, P_{out,j} \text{ and } \dot{m}_j \text{ for } j=2.$$

4. Step 3 is repeated for the third channel, and so on.

The solution would end at the last channel, for which the predicted flow rate should match what is left from an overall mass balance for the entire system. The aforementioned algorithm has been developed, and tested. Numerical tests show that the algorithm converges well. Preliminary application of the model to a test data previously provided to us by Tyndall, however, showed that for the given boundary conditions the total mass flow rate could have been carried through by only about half the channels. This indicates that we may be under estimating the pressure drops in the system. Underestimation of singular pressure losses associated with the numerous bends and turns in the system is of course a potential main contributor. More accurate representation of the entire system geometry is evidently needed.

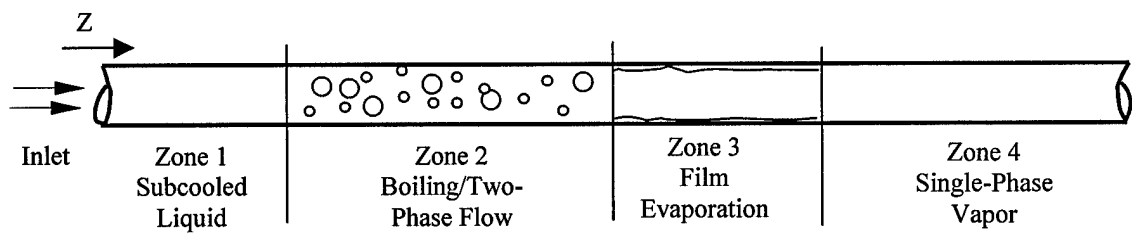


Fig.1 Schematic of a Boiling Channel

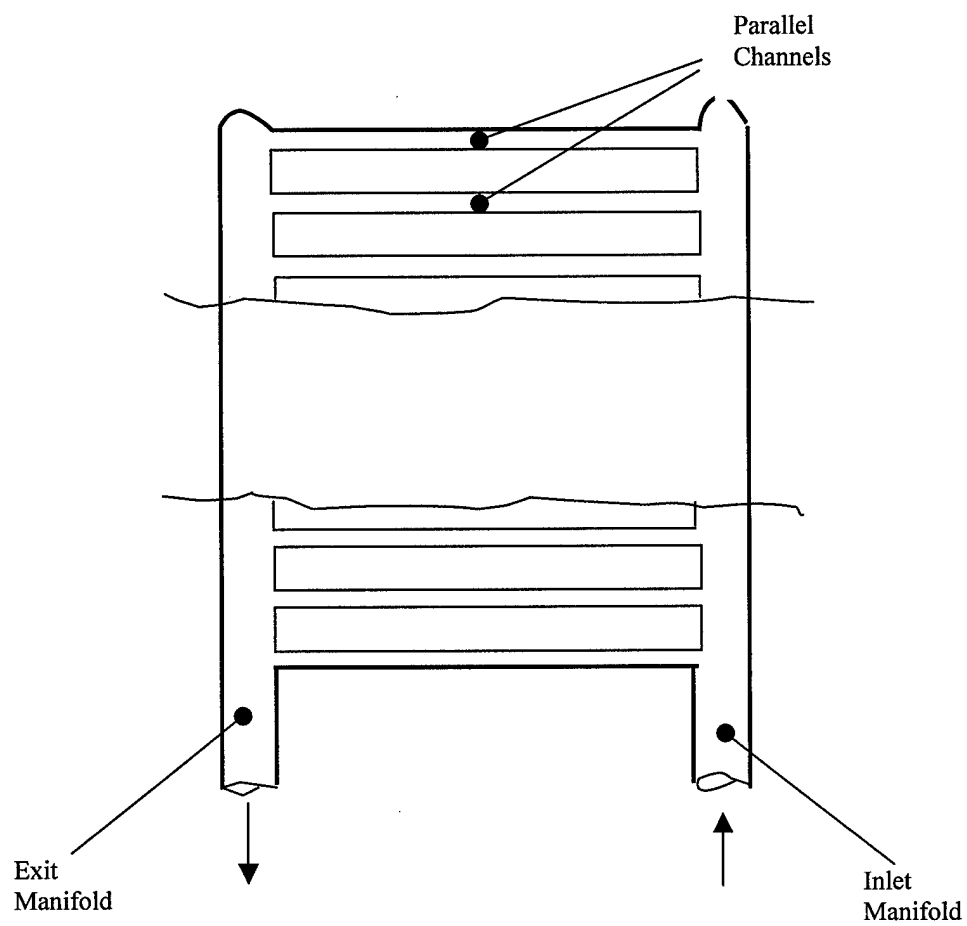


Fig. 2 Schematic of a Multi-Channel Evaporator with Inlet and Exit Manifolds

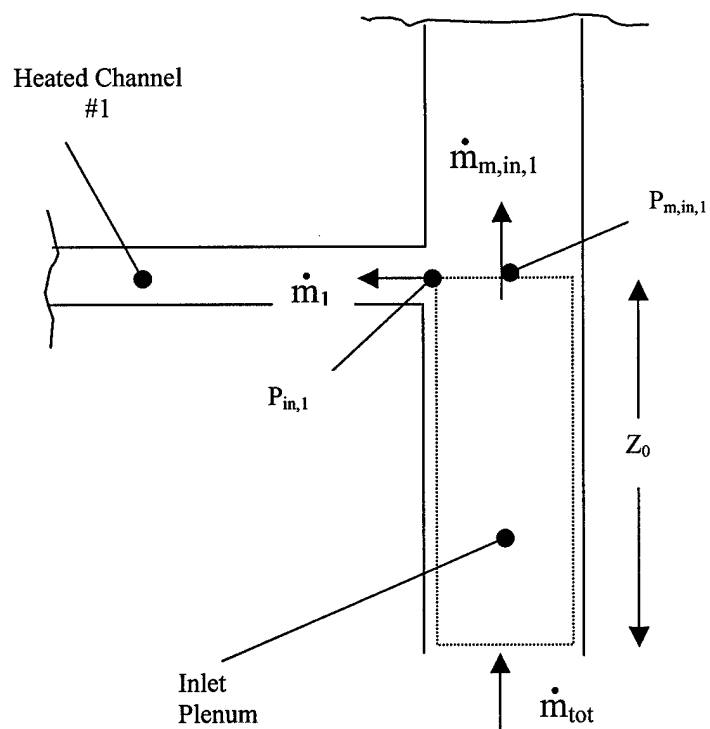


Fig.3 The Control Volume at the Entrance of the Inlet Manifold

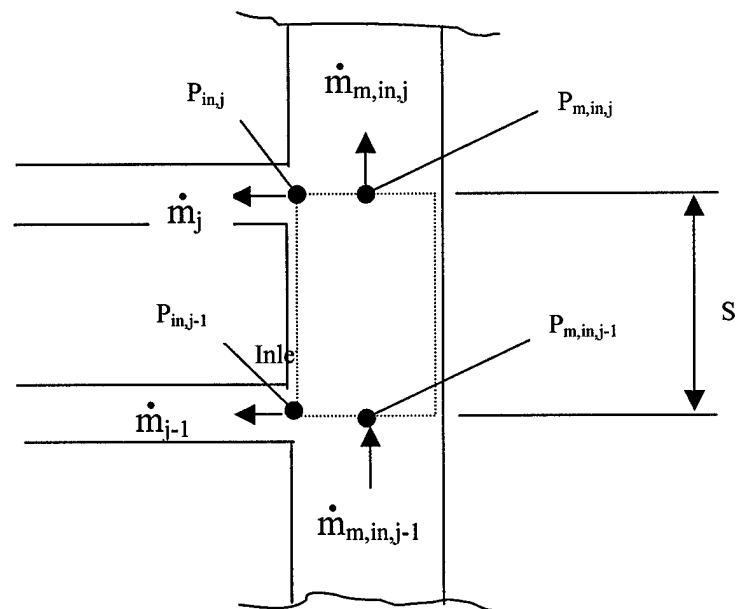


Fig.4 The Control Volume Between Entrances to Channels $j-1$ and j

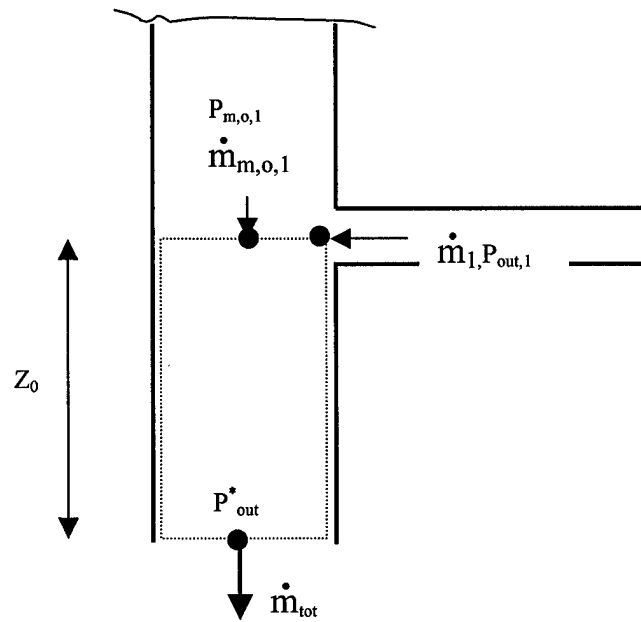


Fig.5 The Control Volume at the Exit of the Exit Manifold

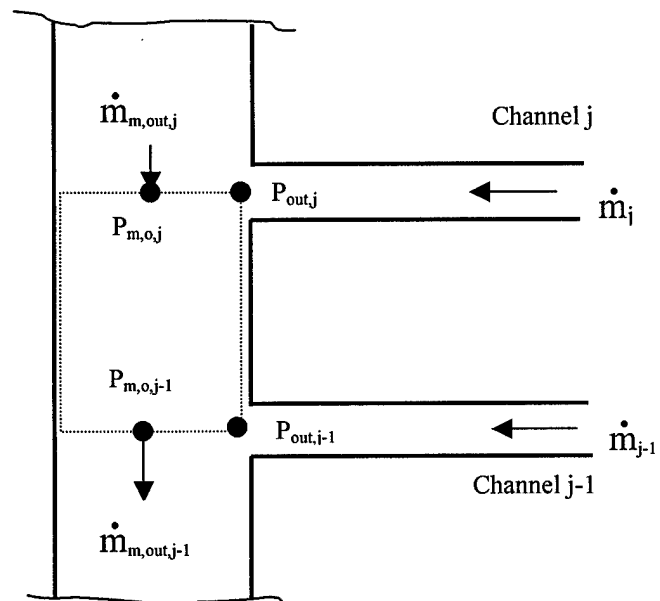


Fig.6 The Control Volume Between Exits of Channels j-1 and j

4.0 Condenser and Moisture Separation Systems

4.1 General Remarks

Efficient and innovative condenser designs are needed for the fuel cells of interest in this study, since the vapor pressure in the vapor noncondensable mixture that should be used for condensation is typically low. Surface condensers, as is well-known, are inefficient when large concentrations of noncondensables are present. For this reason, the condenser systems of interest in the study consist of :

- 1). An expander, in which the vapor-noncondensable is depressurized. Partial condensation of the vapor phase then results, either as a result of fog formation, or as a result of condensation on micro droplets of water that have intentionally been sprayed into the flown field.
- 2). A cyclone-like separator, in which the droplet-laden gas-vapor mixture flows through a tortuous passage. The highly curved streamlines that are imposed on the mixture result in the inertial impaction of the entrained droplets on the walls of the flow passage.

In what follows, engineering models are briefly described, that have been developed for the simulation of a system consisting of an expander with known inlet and exit pressures, and a cyclone-type separator, that are configured in series.

4.2 Expander Models

Four types of expanders are modeled. Expander Types 1 and 4 consist of a system, with or without moving parts, with known inlet and outlet pressures. Expander Types 2 and 3, on the

other hand, are turbine expanders with known input pressures, known power outputs, and known isentropic efficiencies. For these expanders the exit pressure is actually calculated using thermodynamic relations. In Expander Types 1 and 3, furthermore, droplets with a log-normal size distribution at a constant rate are assumed to be injected into the vapor-noncondensable mixture at inlet, in order to act as condensation sites. In Expander Types 2 and 4, however, spontaneous fog formation is assumed to take place.

Common to all of the afore-mentioned expander types are the following assumptions:

1. The system is at steady-state.
2. The vapor-noncondensable mixture and its entrained liquid droplets are everywhere at thermodynamic equilibrium.
3. The gas and liquid droplets everywhere have the same velocity.
4. The liquid condensate is impermeable to the noncondensable.
5. The noncondensable is an ideal gas
6. Except for the inlet and outlet, no mass transfer through the walls of the system takes places
7. Droplet break-up and coalescence are neglected.

4.2.1 Expander Types 1 and 4

First consider the Expander Types 1 or 4. The schematic in Figure 7 represents the modeled system. For this system the following balance equation can be written:

- **Total Mass balances:**

$$A_1 U_1 [(1 - \epsilon_1) \rho_{G,2} + \epsilon_1 \rho_{f,1}] = A_2 U_2 [(1 - \epsilon_2) \rho_{G,2} + \epsilon_2 \rho_{f,2}] \quad (51)$$

where A represents the flow area, U represents velocity, and ϵ represents the in-situ volume fraction occupied by liquid droplets. Subscripts 1 and 2 represent the inlet and exit, respectively. Also, subscript f represents the liquid phase while subscript G represents the vapor noncondensable mixture.

- **Noncondensable Mass Balance:**

$$A_1 U_1 [(1 - \epsilon) \rho_{G,1} x_{n,1}] = A_2 U_2 [(1 - \epsilon_2) \rho_{G,2} x_{n,2}] \quad (52)$$

where x_n in this and the forthcoming equations represents the mass fraction of the noncondensable in the vapor-noncondensable mixture.

- **Mixture Energy Balance:**

$$\begin{aligned} A_1 U_1 \left[(1 - \epsilon_1) \rho_{G,1} \left(h_{G,1} + \frac{1}{2} U_1^2 \right) + \rho_{f,1} \left(h_{f,1} + \frac{1}{2} U_1^2 \right) \right] \\ + \dot{Q} - \dot{W} = A_2 U_2 \left[(1 - \epsilon_2) \left(h_{G,2} + \frac{1}{2} U_2^2 \right) + \epsilon_2 \rho_{f,2} \left(h_{f,2} + \frac{1}{2} U_2^2 \right) \right] \end{aligned} \quad (53)$$

where for the Expander Types 1 and 4 of course $\dot{Q} = \dot{W} = 0$.

Alternatively, the above equations can be replaced with the following equations

- **Total Mass Balance:**

$$A_2 U_2 [(1 - \epsilon_2) \rho_{G,2} + \epsilon_2 \rho_{f,2}] = \dot{m}_{G,1} + \dot{m}_{f,1} \quad (54)$$

where:

$$\dot{m}_{G,1} = \dot{m}_{v,1} + \dot{m}_{n,1} \quad (55)$$

$$\dot{m}_G = \text{mass flow rate vapor and noncondensable}$$

$$\dot{m}_v = \text{vapor mass flow rate}$$

$$\dot{m}_n = \text{noncondensable mass flow rate}$$

\dot{m}_f = liquid mass flow rate

Note that everywhere:

$$\dot{m}_n = \dot{m}_G x_n \quad (56)$$

- **Noncondensable Mass Balance:**

$$A_2 U_2 \left[(1 - \epsilon_2) \rho_{G,2} x_{n,2} \right] = \dot{m}_{G,1} x_{n,1} = \dot{m}_{n,1} \quad (57)$$

- **Mixture Energy Balances:**

$$\begin{aligned} & A_2 U_2 \left[(1 - \epsilon_2) \rho_{G,2} \left(h_{G,2} + \frac{1}{2} U_2^2 \right) + \epsilon_2 \rho_{f,2} \left(h_{f,2} + \frac{1}{2} U_2^2 \right) \right] \\ &= \dot{Q} - \dot{W} + \dot{m}_{v,1} h_{g,1} + \dot{m}_{n,1} h_{n,1} + \dot{m}_{G,1} \frac{1}{2} U_1^2 + \dot{m}_{f,1} h_{f,1} \end{aligned} \quad (58)$$

Knowing all inlet parameters, and assuming that P_2 is also known, Eqn. (50-52), or alternatively Eqns. (53-57), with appropriate constitutive relations, must be solved in order to obtain, $\epsilon_2, h_{G,2}, h_{f,2}, U_2$, and $x_{n,2}$. The constitutive relations will be described in the forthcoming Sect 4.2.3.

For the Expander Type 1, at inlet, droplets with a log-normal size distribution, at a total mass flow rate of $\dot{m}_{f,1}$ and at a total number rate of $\dot{N}_{f,1}$ and at a total number rate of $\dot{N}_{t,1}$ are injected into the flow field.

The log-normal size distribution, which is likely to apply to spray droplets, can be represented as:

$$\frac{N(D)}{N_t} = F(D) = \frac{1}{\ln \sigma_g \sqrt{2\pi} D} \exp \left[-\frac{(\ln D - \ln \bar{D})^2}{2 (\ln \sigma_g)^2} \right] \quad (57-a)$$

where:

$N(D)dD =$ number density of droplets with diameters in the D to $D+dD$ range

$N_t =$ total number density of droplets

$\sigma_g =$ geometric standard deviation

obviously,

$$\epsilon = \int_{D=0}^{\infty} \frac{\pi}{6} D^3 f(D) dD \quad (59)$$

The droplet (number) average and volume (or mass) average diameter, \bar{D} , and \bar{D}_v , respectively, are defined as

$$\bar{D} = \int_0^{\infty} f(D) D dD \quad (60)$$

$$\bar{D}_v^3 = \int_0^{\infty} f(D) D^3 dD \quad (61)$$

It can also be shown that for the log-normal size distribution:

$$\ln \bar{D}_v = \ln \bar{D} + 3(\ln \sigma_g)^2 \quad (62)$$

We assume that, as a result of condensation, the droplets grow in size such that the size distribution function does not change (i.e., it remains log-normal, with the geometric standard deviation unchanged). As a result, the volume-average droplet diameter at exit will be

$$\bar{D}_{v2} = \left(\frac{6 \epsilon_2}{\pi N_{t,2}} \right)^{1/3} \quad (63)$$

Note that the conservation of droplet number requires that

$$A_1 U_1 N_{t,1} = A_2 U_2 N_{t,2} \quad (64)$$

An equation similar to Eqn. (63) can obviously be also written for the inlet to the expander.

For the Expander Type 4, Eqns. (53,-57) apply, except that now $\dot{m}_{f,1} = 0$. Also, for this expander type, the droplet volume-averaged diameter should be provided by the user. Knowing $\bar{D}_{v,2}$, the number density and number flow rate can be easily calculated.

4.2.2 Expander Types 2 and 3

These expander types, as mentioned earlier, are actually adiabatic turbine expanders with known isentropic efficiency η_T , where:

$$\eta_T = \dot{W} / \dot{W}_s \quad (65)$$

where \dot{W} and \dot{W}_s represent the turbine power, and its isentropic power, respectively.

For these expanders, first \dot{W}_s is calculated. The calculated \dot{W} is then used in Eqn. (64), and \dot{W} is found. Subsequently, Eqns. (53-57), along with the constitutive relations describe in the next section, are solved.

To obtain \dot{W}_s , the following is done. In Eqn. (57), \dot{W} is replaced with \dot{W}_s . Equations (53-57) are then solved, along with the following equation which ensures an isentropic expansion of the fluid mixture in the expander:

$$\dot{m}_{v,1}s_{g,1} + \dot{m}_{n,1}s_{n,1} = A_2 U_2 \left[(1 - \epsilon_2) s_{G,2} + \epsilon_2 s_{f,2} \right] \quad (66)$$

$$s_{f,1}, s_{g,1} = \text{saturated water and vapor entropies at inlet}$$

$$s_{f,2} = \text{saturated water entropy at exit (for the vapor partial pressure at exit)}$$

$$s_{G,2} = \text{vapor-non condensable mixture entropy}$$

Note that

$$s_{G,2} = x_{n,2}s_{n,2} + (1-x_{n,2})s_{g,2} \quad (67)$$

Iterative solution of the above equations, along with other appropriate constitutive relations, leads to the calculation of \dot{W}_s , as well as the isentropic values of $\epsilon_2, h_{G,2}, h_{f,2}$, etc. Only \dot{W}_s is useful, however.

4.2.3 Constitutive Relations

These relations apply to the expander inlet, outlet, or anywhere else in the flow field.

$$P = P_v + P_n \quad (68)$$

where

P = Total local pressure

P_v, P_n = Vapor and noncondensable partial pressures, respectively

$$P_n = Y_n P \quad (69)$$

$$Y_n = \frac{\frac{x_n / M_n}{\frac{x_n}{M_n} + \frac{1-x_n}{M_v}} \quad (70)$$

where:

Y_n = mole fraction of noncondensable

M_n, M_v = molar masses of noncondensable and vapor respectively

$$T = T_{sat}(P_v) \quad (71)$$

$$\rho_G = \rho_g(P_v) + \frac{P_n}{\frac{R}{M_n} T} \quad (72)$$

R = universal gas constant

ρ_g = saturated vapor density

$$h_G = (1 - x_n)h_g + x_n h_n(T) \quad (73)$$

where:

h_n = Specific enthalpy of the noncondensable species

Also, since we treat the noncondensable (air in this case) as an ideal gas, can write:

$$s_{n,2} - s_{n,1} = s_n^o(T_2) - s_n^o(T_1) - \frac{R}{M_n} \ln \left(\frac{(1 - x_{n,2})P_2}{(1 - x_{n,1})P_1} \right) \quad (74)$$

where $s_n^o(T_2)$ and $s_n^o(T_1)$ are the following standard function

$$s_n^o(T) = \int_o^T C_{pn} \frac{dT}{T} \quad (75)$$

Values of $s_n^o(T)$ for air were calculated by interpolation using the tables of Black and Hartley (1996).

4.2.4 Solution Method

For each expander type, the relevant set of algebraic equation for is a closed, non-linear equation system. These equations are solved using the Newton iteration method. Briefly, for the equation:

$$f(x) = 0 \quad (76)$$

the iterations in search of the roots of Eqn. (75) follow:

$$x_{n+1} = x_n - f(x_n) / f'(x_n) \quad (77)$$

where subscripts n and $n+1$ represent their respective iteration levels, and f' is the derivative of $f(x)$ with respect to x .

When a set of nonlinear equations are dealt with, Eqn.(76) is replaced with

$$X_{n+1} = X_n - F(X_n)/J \quad (78)$$

where X now represents a column vector with elements x_1, x_2, \dots , and $F(X)$ is a column vector with elements $f_1(x_1, x_2, \dots), f_2(x_1, x_2, \dots)$, etc., and parameter J is the determined of the Jacobian matrix. The elements of the Jacobian matrix are themselves approximately obtained from

$$\frac{\partial f_i}{\partial x_j} = \frac{f_i(x_j + H) - f_i(x_j)}{H} \quad (79)$$

where H is a small number.

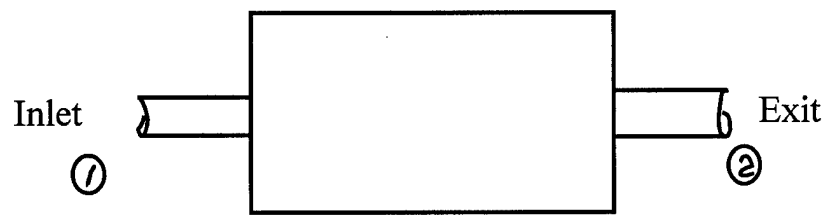


Fig.7 Schematic of Expander Types 1 or 4

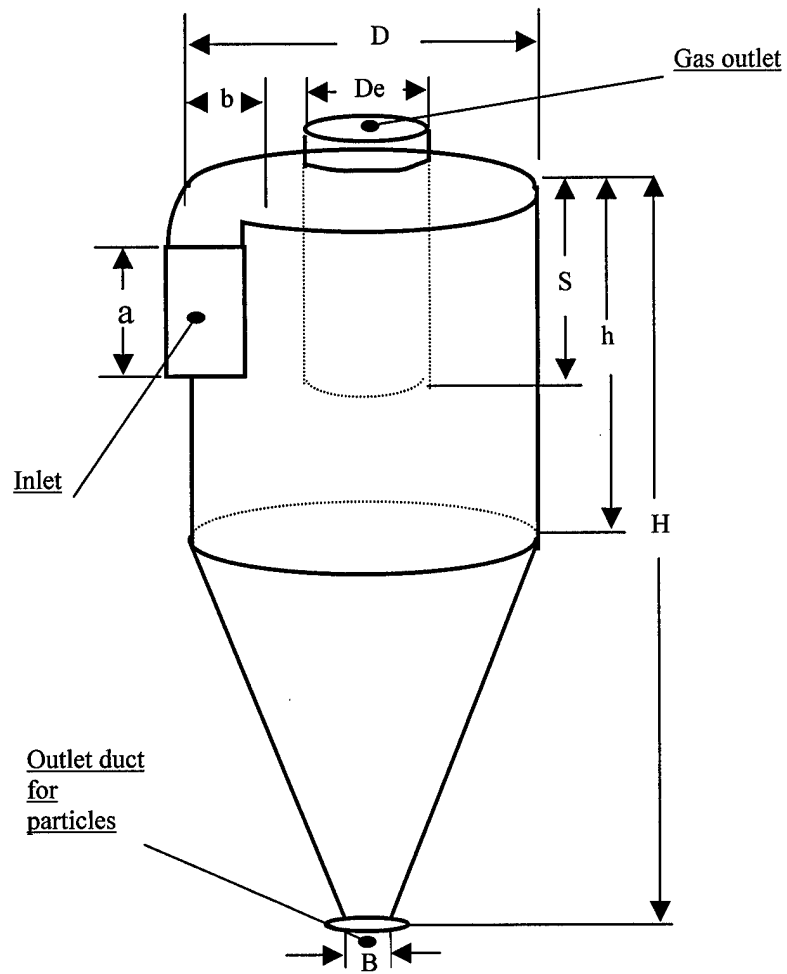


Fig. 8 Schematic of a cyclone with Tangential Gas Inlet (Leith and Licht, 1972)

4.3 Cyclone-Type Separator

4.3.1 General Remarks

Cyclone separators are devices that partially remove particles suspended in a particle-laden gas or liquid. Particle removal is achieved by providing a highly curved flow path for the fluid mixture. Unless the particles are neutrally-buoyant, they would deviate from the carrier fluid's stream lines due to their inertia, and particle-wall impactions would result in the removal of particles from the mixture.

Cyclone separators and their hydrodynamic and particle transport characteristics have been extensively studied in the past. Earlier modelers attempted to derive closed mathematical expressions or simple numerical methods for calculating the removal or collection efficiency of cyclones with known geometric configurations. CFD-type models, which can address cyclone separators with rather arbitrary geometric configurations, have been developed and published more recently. Virtually all published studies, however, are concerned with particles that do not undergo phase change. A brief review of the recent literature follows.

An important, widely-used simple model for the collection efficiency of cyclones is the model of Leith and Licht (1972). The configuration of a cyclone with tangential gas inlet, modeled by the latter authors, is shown schematically in Fig. 8. The semi-mechanistic model of Leith and Licht can also be applied to cyclones with circular inlets. Other, more recent studies dealing with cyclones include the following. Comas et al. (1991) experimentally studied the effect of dust and inlet vanes on cyclone collection efficiency and pressure drop. Dust particles reduced pressure drop, while vanes reduced the removal efficiency and pressure drop both.

Dyakowski and Williams (1993) numerically modeled the flow in narrow hydrocyclones, using the $k-\epsilon$ turbulence model. Griffith and Boysan (1996) argued that cyclone models such as the model of Leith and Licht (1972) are good for large, industrial cyclones, and may not be appropriate for small units. They performed CFD-type analysis of three model cyclone types and assessed the performance of three relevant empirical models. Hoekstra et al. (1999) performed an experimental and numerical study of turbulent flow in a gas cyclone. In their CFD analysis, they compared the performance of three different turbulence models, showing that the RSM performed better than the $k-\epsilon$ and RNG models. Chmielniak and Bryczkowski (2000) presented a theoretical model for a patented cyclone device which employs swirling baffles and a bottom clean gas take-off. Their theoretical model was based on the modification of the aforementioned model of Leith and Licht (1972).

A simple, one-dimensional model based on the assumption of a spiral motion with constant acceleration in the cyclone has also been suggested recently (Avci and Karagoz, 2000). However, it has not been sufficiently validated against experimental data.

As noted earlier, the above studies as well as others in the open literature, are primarily concerned with particles without phase change. The physical situation we deal with is different, however. The vapor-noncondensable-droplet mixture undergoes depressurization in the cyclone, which results in further condensation of vapor on droplets, the growth of droplets size, and the reduction of the mixture mean velocity. In addition, the geometric configuration of the cyclone of interest may not exactly coincide with the standard cyclone depicted in Fig. 8.

Detailed CFD-type analysis is evidently needed for cases of interest here, and should be performed in the future. At this point, however, in light of the uncertainties regarding the final separator design, only a simple model will be developed.

4.3.2 Cyclone Model

The cyclone separator model will be based on modification of the model of Leith and Licht (1972), in order to account for: (a) the occurrence of condensation during the flow in the cyclone; and (b) the geometric difference (primarily the absence of the conic part. see Fig. 8.) between the currently selected design and the cyclone model by the latter authors.

The modified model, in addition to the assumptions that are the bases of the model of Leith and Licht (1972), assumes the following.

1. At inlet to the cyclone the particle size distribution, along with other flow parameters, are all known.
2. The vapor-noncondensable-droplet mixture is at thermodynamic equilibrium everywhere in the system.
3. For particle removal calculations the particles can be treated as monodisperse, with the volume-average diameter as their effective diameter.
4. The removal (collection) efficiency of the cyclone can be obtained using the method of Leith and Licht, based on the particle size characteristics midway in the cyclone.
5. The collected droplets all leave the cyclone as saturated liquid corresponding to the cyclone exit pressure.

The cyclone performance is accordingly obtained by the simultaneous solution of overall mass and energy balance equation, along with the expressions from Leith and Licht model. The set of coupled equations are as follows.

- **Mixture Mass Balance**

$$\dot{m}_{rem} + A_2 U_2 \left[(1 - \epsilon_2) \rho_{G,2} + \epsilon_2 \rho_{f,2} \right] = \dot{m}_{G,1} + \dot{m}_{f,1} \quad (80)$$

- **Noncondensable Mass Balance**

$$A_2 U_2 \left[(1 - \epsilon_2) \rho_{G,2} x_{n,2} \right] = \dot{m}_{n,1} \quad (81)$$

- **Mixture Energy Balance**

$$\begin{aligned} \dot{m}_{rem} h_{f,2} + A_2 U_2 \left[\rho_{G,2} (1 - \epsilon_2) \left(h_{G,2} + \frac{1}{2} U_2^2 \right) \right. \\ \left. + \epsilon_2 \rho_{f,2} \left(h_{f,2} + \frac{1}{2} U_2^2 \right) \right] = \dot{m}_{v,1} h_{g,1} + \dot{m}_{n,1} h_{n,1} \\ + \dot{m}_{G,1} \frac{1}{2} U_1^2 + \dot{m}_{f,1} h_{f,1} \end{aligned} \quad (82)$$

where the removed liquid flow rate is given by:

$$\dot{m}_{rem} = (N_1 A_1 U_1 - N_2 U_s A_2) \rho_f \frac{\pi}{6} \bar{D}_v^3 \quad (83)$$

where N_1 and N_2 are droplet number densities at inlet and exit, respectively. Also,

$$\bar{D}_v = \frac{1}{2} (\bar{D}_{v1} + \bar{D}_{vs}) \quad (84)$$

$$N_2 = N_1 (1 - \eta) \quad (85)$$

$$\epsilon_2 = N_2 \frac{\pi \bar{D}_{v2}^3}{6} \quad (86)$$

The collection efficiency, η , is now formulated following Leith and Licht (1972)

(see Fig.8 for the definition of geometric parameters used):

$$\eta = 1 - \exp \left[-2c(\psi)^{\frac{1}{2n+2}} \right] \quad (87)$$

$$c = \frac{8k_c}{k_a k_b} \quad (88)$$

$$\psi = \frac{\rho_p d_p^2 U_{T_2}}{18\mu D} (n+1) \quad (89)$$

where V_s is the annular shape volume above the exit duct through the mid-level of the entrance duct, and:

$$U_{T_2} = U_1 \quad (90)$$

$$V_H = (h-s) \cdot \frac{\pi}{4} D^2 \quad (91)$$

$$n = \frac{(12D_f)^{0.14}}{2.5} \quad (92)$$

$$V_H = (h-s) \frac{\pi}{4} D^2 \quad (93)$$

$$k_a = \frac{a}{D} \quad (94)$$

$$k_b = \frac{b}{D} \quad (95)$$

$$k_c = \frac{V_s + \frac{1}{2} V_H}{D^3} \quad (96)$$

It should be mentioned that in the method of Leith and Licht, a natural length, l , and a corresponding volume V_{nl} and k_c are defined as:

$$l = 2.3D_e (D^2 / ab)^{1/3} \quad (97)$$

$$V_{nl} = l \frac{\pi}{4} D^2 \quad (98)$$

$$k_c = \frac{V_s + \frac{1}{2} V_{nl}}{D^3} \quad (99)$$

Since our current separator design does not include a conical segment, we have defined k_c according to Eqn. (94).

Also, when the inlet to the cyclone is circular rather than rectangular, the above equations apply as long as ab is replaced with the cross-sectional area of the inlet channel, and $k_a k_b$ is replaced with $\pi/4 (D_i/D)^2$, with D_i representing the inlet channel diameter.

5.0 References

- Al-Johani, M. S., 1995, "A Three-Dimensional Mechanistic Model of Steam Condensers Using Porous Medium Formulation," Ph.D. Thesis, Georgia Institute of Technology, Atlanta, GA.
- Ali, M. I., and Kawaji, M., 1991, "The Effect of Flow Channel Orientation on Two-Phase Flow in a Narrow Passage between Flat Plates," *Proc. ASME/JSME Thermal Eng. Conf.*, Vol. 2, pp. 183-190.
- Ali, M. I., Sadatomi, M., and Kawaji, M., 1993, "Adiabatic Two-Phase Flow in Narrow Channels between Two Flat Plates," *Can. J. Chem. Eng.*, Vol. 71- pp. 657-666.
- Avci, A., and Karogoz, I., 2000, "A Mathematical Model for the Determination of a Cyclone Performance," *Int. Comm. Heat. Mass Transfer*, Vol. 27 pp.253-272
- Awwad, A., Rodriquez, J., Xin, R. C., Dong, Z. F., and Ebadian, M. A., 1994, "Heat Transfer of Air/Water Two-Phase Flow in a Helicoidal Pipe," *NE-Vol. 15, Thermal Hydraulic of Advanced Steam Generators and Heat Exchanges*, pp. 73-80, ASME.
- Awwad, A., Xin, R. C., Rodriguez, J. Dong, Z. F., Ebadian, M. A., and Soliman, H. M., 1994, "Flow Pattern and Pressure Drop in Air-Water Two-Phase Flow in the Horizontal Helicoidal Pipe," *HTD-Vol. 271, General Papers in Heat and Mass Transfer. Insulation and Turbomachinery*, pp. 97-104, ASME.
- Awwad, A., Xin, R. C., Dong, Z. F., Ebadian, M. A., and Soliman, H. M. , 1995, "Measurement and Correlation of the Pressure Drop in Air-Water Two-Phase Flow in Horizontal Helicoidal Pipes," *Int., J. Multiphase Flow*, Vol. 21, pp. 607-619.
- Banerjei, S., Rhodes, E., and Scott, D. S., 1969, "Studies on Cocurrent Gas-Liquid Flow in Helically Coiled Tubes – I. Flow Patterns, Pressure Drop and Holdup," *Can, J. Chem. Eng.*, Vol. 47, pp 445-453
- Beattie, D. R. H., and Whalley, P. B., 1982, "A Simple Two-Phase Frictional Pressure Drop Calculation Method," *Int. J. Multiphase Flow*, Vol. 8, pp. 83-87.
- Black, W. Z., and Hartley, J. G., 1996, *Thermodynamics*, 3rd ed., Harper Collins, New York.
- Chisholm, D., and Laird, A. D. K., 1958, "Two-Phase Flow in Rough Tubes," *Trans. ASME*. Vol. 80, pp. 276-283
- Chmielniak, T., and Bryczkowski, A., 2000, "Method of Calculation of New Cyclone- Type Separator with Swirling Battle and Bottom Take off of Clean Gas-Part I: Theoretical Approach," *Chem. Eng. Sci.*, Vol. 55 pp 441-448
- Comas, M., Comas, J., Chetrit, C., and Casal, Jr., 1991, "Cyclone Pressure Drop and Efficiency With and Without an Inlet Value," *Powder Technology*, Vol. 66, pg. 143-148.

Dyakowski, T., and Williams, R. A. , 1993, "Modeling Turbulent Flow Within a Small-Diameter Hydroclone," *Chem. Eng. Sci.*, Vol. 48, pp. 1143-1152

Ekbert, N. P., Ghiaasiaan, S. M., Abdel-Khalik, S. I., Yoda, M., Jeter, S.M. 1999, "Gas-Liquid Two-Phase Flow in Narrow Horizontal Annuli," *Nucl. Eng. Design*, Vol. 192, pp. 59-80.

Fourar, M., and Bories, S., 1995, "Experimental Study of Air-Water Two-Phase Flow through a Fracture (Narrow Channel)," *Int. J. Multiphase Flow*, Vol. 21, pp. 621-637.

Ghiaasiaan, S. M., and Geng, H., 1997, "Mechanistic Non-Equilibrium Modeling of Critical Flashing of Subcooled Liquids Containing Dissolved Noncondensables," *Num. Heat Transfer* Vol. B32, pp. 435-457

Ghiaasiaan, S. M., and Abdel-Khalik, S. I., 2000, "Two-Phase Flow in Microchannels," *Advances in Heat Transfer*, Vol. 34, pp. 145-254.

Ghiaasiaan, S. M., Kamboj, B. K., and Abdel-Khalik, S. I., 1995, "Two-Fluid Modeling of Condensation in the Presence of Noncondensables in Two-Phase Channel Flows," *Nuclear Science and Engineering*, Vol., 119, pp. 1-17.

Ghiaasiaan, S. M., Wassel, A. T., and Lin, C. S., 1991, "Direct Contact Condensation in the Presence of Noncondensables in OC-OTEC Condensers," *J. Solar Energy Eng.*, Vol. 113, pp. 228-235.

Griffith, W. D., and Boysan, F., 1996, "Computational Fluid Dynamics (CFD) and Empirical Modelling of the Performance of a Number of Cyclone Samplers," *J. Aerosol Sci.*, Vol. 27, pp. 281-304

Grigull, V., Straub, J., and Schiebener, P., eds., 1984, *Steam Tables in SI Units*, Springer-Verlag, New York.

Hindmarsh, A. C., Dec. 1980, "LSODE and LSODI, Two New Initial Value Ordinary Differential Equation Solvers," *ACM Newsletter*, Vol. 15, 4, p. 10

Hoekstra, A.J., Derksen, J.J. and Van Den Akker, H. E. A., 1999, "An Experimental and Numerical Study of Turbulent Swirling Flow in Gas Cyclones," *Chem. Eng. Sci.*, Vol. 54, pp. 2055-2065.

Ito, H., 1959, "Friction Factors for Turbulent Flow in Curved Pipes," *J. Basic Eng.*, pp. 123-134.

John, H., Reimann, J., Westphal, F., and Friedel, L., 1988, "Critical Two-Phase Flow through Rough Slits," *J. Int. J. Multiphase Flow*, Vol. 14, pp. 155-174.

Jones, O. C. Jr., 1976, "An Improvement in the Calculation of Turbulent Friction in Rectangular Ducts," *Fluids Eng.*, Vol. 98, pp. 173-181.

Kakac, S., Shah, R. K., and Aung, W., 1987, *Handbook of Single-Phase Convective Heat Transfer*, Wiley, New York.

Kaji, M., Mori, K., Nakanishi, S., and Ishigai, S., 1984, "Flow Region Transitions for Air-Water Flow in Helically Coiled Tubes," *Mult-Phase Flow and Heat Transferr III, Part A: Fundamentals*, Elsevier, Amsterdam.

Kang, H. J., Lin, C.X., and Ebadian, M. A., 2000, "Condensation of R134a Flowing Inside Helicoidal Pipe," *Int. J. Heat Mass Transfer*, Vol. 43, pp. 2553-2564.

Kuck, I. Z., 1982, "Thermodynamic Properties of Water for Computer Simulation of Power Plants," Department of Nuclear Engineering, The University of Arizona, Tucson. Prepared for Division of Accident Evaluation Office of Nuclear Regulatory Research, U. S. Nuclear Regulatory Commission, Washington, D. C., NRC FIN A4065.

Leith, D., and Licht, W. 1972, "The Collection Efficiency of Cyclone Type Particle Collectors – A New Theoretical Approach," *AIChE Symp. Ser.* 68, No. 126, pp. 196-206

Li, L. J., Lin, C. X., and Ebadian, M. A., 1998 "Turbulent Mixed Convective Heat Transfer in the Entrance Region of a Curved Pipe with Uniform Wall-Temperature," *Int. J. Heat Mass Transfer*, Vol. 41, pp. 3793-3805.

Lin, C.X., and Ebadian, M. A. , 1997, "Developing Turbulent Convective Heat Transfer in Helical Pipes," *Int. J. Heat Mass Transfer*, Vol 40, pp. 3861-3873

Manlapaz, R. L., and Churchill, S. W., 1980, "Fully-Developed Laminar Flow in a Helically Coiled Tube of Finite Pitch," *Chem. Eng. Comm.*, Vol. 7, pp. 57-78.

Mishima, K., Hibiki, T., and Nishihara, H., 1993, "Some Characteristics of Gas-Liquid Flow in Narrow Rectangular Ducts," *Int. J. Multiphase Flow*, Vol. 19, pp. 115-124.

Press, W. H., Flannery, B. P., Teukolsky, S. A., and Vetterling, W. T., 1988, *Numerical Recipes – The Art of Scientific Computing*, Cambridge University Press, Cambridge, U.K., p. 80.

Saxena, A. K., Schumpe, A., Nigam, K.D.P., and Deckwer, W.D., 1990, "Flow Regimes, Hold-up and Pressure Drop for Two-Phase Flow in Helical Coils," *Can. J. Chem. Eng.*, Vol. 68, pp. 553-559

Wilmarth, T., and Ishii, M., 1994, "Two-Phase Flow Regimes in Narrow Rectangular Vertical and Horizontal Channels," *Int. J. Multiphase Flow*, Vol., 37, pp. 1749-1758.

Xin, R. C., Awwad, A., Dong, Z. F., and Ebadian, M. A., 1996, "An Investigation and Comparative Study of the Pressure Drop in Air-Water Two-Phase Flow in Vertical Helicoidal Pipes," *Int. J. Heat Mass Transfer*, Vol. 39 pp. 735-743.

Appendix A

EVAPMC: A Computer Code for the Analysis of Evaporation in Small Flow Passages

Authors

S. M. Ghiaasiaan
B.N. McCord

Submitted by:

G.W. Woodruff School of Mechanical Engineering
Georgia Institute of Technology
Atlanta, GA 30332-0405

Submitted to:

Tyndall Air Force Base
FL 32403-5526

January 18, 2002

Table of Contents

Section	Page
Table of Contents	
1. Introduction	
1.1 Problem Background	
1.2 Report Summary	
2. Description of the Theory	
3. Code Structure	
4. Description of Subroutines and Functions	
5. Input and Output	
6. Sample Run	

Section 1 Introduction

1.1 Problem Background

EVAPCM is a computer code that has been developed to mechanistically model the evaporator process in a uniform cross-section channel. EVAPCM is based on the numerical solution of sets of one-dimensional conservation equations in various segments of a boiling channel (the subcooled segment near the inlet, the two-phase boiling segment, etc.), everywhere using appropriate closure relations, and is capable of providing hydrodynamic details of the flow field it models.

EVAPCM contains built-in closure relations that are suitable for the analysis of the evaporation of water in a small flow passage with rectangular cross-section. Extensive property routines for water are included in the code. The mechanistic modeling approach, however, is quite general, and constitutive relations suitable for other configurations and working conditions can be easily incorporated into the code.

1.2 Report Summary

Section 2 briefly describes the phenomena that are modeled in this computer code. The code structure along with its flow diagram is presented in Section 3. Section 4 briefly describes each of the routines used in the code. The input and output are described in Section 5. A sample case is provided in Section 6, where a complete listing of all the input and output is included. The references are listed in Section 7.

Section 2

Description of the Theory

The modeled flow channels can be divided into 4 segments, as shown in the schematic in Figure 2.1. The model uses a separate set of steady-state, one-dimensional conservation equations in each region.

In region I, the subcooled liquid region, momentum and energy conservation ordinary differential equations are numerically solved, using pressure and enthalpy as the state variables, until saturation is reached, i.e., until the fluid enthalpy falls below the saturated liquid enthalpy associated with the local pressure. To avoid numerical problems, however, we allow the code to slightly "undershoot". Thus, evaporation is assumed to start when the local equilibrium vapor quality corresponds to a homogeneous void fraction of 0.25%. Once the latter condition is satisfied, Region II starts.

Region II represents the segment of the channel where two-phase flow with various familiar regimes takes place. In this region the separated (two-fluid) conservation equations are numerically solved. It is assumed that the liquid and vapor phases remain at thermodynamic equilibrium, while maintaining different velocities. A simple flow regime map, composed of bubbly, intermittent (churn-slug) and annular flow patterns, is used for the calculation of the interfacial forces. The parameters in each flow regime (e.g., bubble size in bubbly flow) are currently represented with the rectangular channel restrictions in mind. These parameters, however, can be easily modified. The ordinary differential conservation equations are numerically integrated, with pressure, vapor velocity, liquid velocity, and void fraction, as the state variables. Region II is assumed to end when the local equilibrium quality exceeds 20%, and the local void fraction predicted by the two-fluid model exceeds 95%.

Region III represents evaporation in a high-quality two-phase flow pattern, which, based on the phenomenology of boiling in large channels, is likely to represent the annular or annular/mist flow pattern. In this region thermodynamic equilibrium is assumed between the two phases, and the mixture mass, momentum, and energy ordinary differential equations are numerically solved, with pressure, equilibrium quality, and vapor velocity. The velocity slip between the two phases is accounted for by using a correlation due to Zivi (1964), which has been derived based on the assumption of minimum entropy generation in annular flow. Region III is assumed to end when the local equilibrium quality reaches 0.999.

Region IV represents superheated pure vapor. The conservation equations and the solution method are similar to Region I, with compressibility of the vapor phase being the major difference between the two cases.

It should be mentioned that not all the aforementioned regions have to occur in a simulation run. Thus, for example, Region IV will not occur if the exit of the channel is reached before the equilibrium quality reaches 0.999.

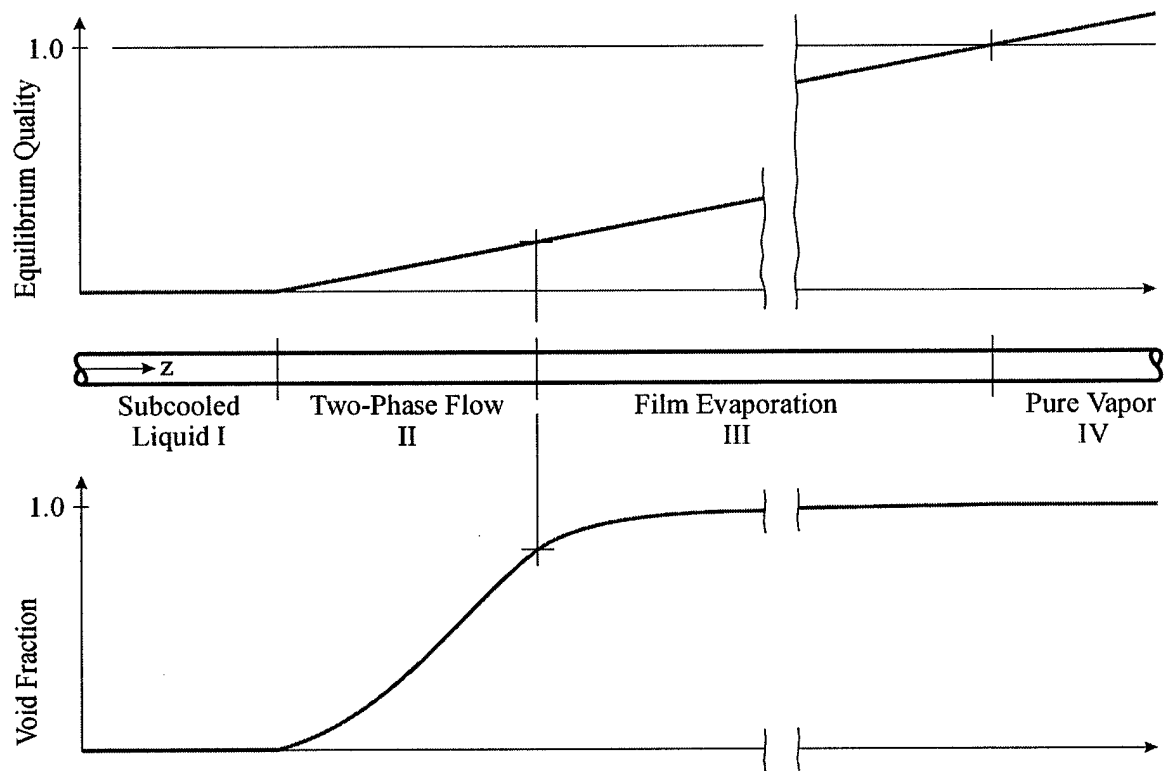


Figure 2.1 Schematic of the Modeled Channel.

Section 3

Code Structure

The logical flow of the computer code is shown schematically in Figure 3-1. The program begins by reading and writing the input data. Following this, the variables that depend on the axial coordinate, z , are initialized. Then the program begins marching down the axial coordinate, in the direction of increasing z . Marching along z in the aforementioned Region I (See Figure 2.1) is performed in subroutine MARCH. Once the criterion for the onset of two-phase flow is reached, the program switches to subroutine MARCH2, where Regions II and III are addressed. Finally, once complete evaporation occurs, the program switches to subroutine MARCH3, where Region IV is addressed, until the channel exit is reached..

A summary of the calculation results is printed at user-specified intervals.

Section 4

Description of Subroutines and Functions

This section contains a description of each subroutine and function contained in this computer code.

Subroutines

CPLT	Finds the subcooled liquid water specific heat given the pressure and temperature.
DVODE	Solves initial-value problems represented by sets of ordinary differential equations. Stiff and non-stiff systems can both be efficiently solved.
FRIEDEL	Calculates the two-phase wall friction using Friedel's (1977) model. (This subroutine is not used at this time.)
FUNC	Calculates and sets up the matrix elements, and performs necessary matrix inversions, for the ode's to be solved in MARCH subroutine.
FUNC2	Calculates and sets up the matrix elements, and performs necessary matrix inversions, for the ode's to be solved in MARCH2 subroutine for Region II.
FUNC2F	Calculates and sets up the matrix elements, and performs necessary matrix inversions, for the ode's to be solved in MARCH2 subroutine for Region III.
FUNC3	Calculates and sets up the matrix elements, and performs necessary matrix inversions, for the ode's to be solved in MARCH3 subroutine.
INVER	This subroutine inverts a matrix using a standard Gauss-Jordan elimination technique.
MARCH	The main routine for Region I calculations.
MARCH2	Main routine for the calculations for Regions II and III.
MARCH3	Main routine for the calculations for Region IV.
POLINT	This subroutine is a Lagrangian interpolation routine, and is used to interpolate between thermodynamic values in property tables.
PRPSAT	A block of subroutines and functions that calculate various water and steam properties at saturated conditions.

PSATF	Finds the saturation pressure given the temperature.
RKAMS	This subroutine is a fixed-step, 4 th order Runge-Kutta solver for ordinary differential equations. It is utilized in MARCH, MARCH2 and MARCH3 routines for the integration of all of the ordinary differential equation sets. (Not used.)
THCND	Finds the thermal conductivity of water using temperature and density.
THCONV	Finds vapor thermal conductivity given pressure and temperature.
VISCOL	Finds the viscosity of water given the saturation temperature.
VISCOV	Finds vapor viscosity given pressure and temperature.

Functions

CPA28	Finds the specific heat of N_2 gas (not used here).
CPGAS	Finds the specific heat at constant pressure for superheated steam given the temperature.
CPVPT	Finds the specific heat of water vapor given pressure and temperature.
DHGPSAT	Finds the derivative of enthalpy versus pressure for water vapor.
EKNTHE	Finds thermal conductivity for non-condensable He, given the temperature.
EMUNTHE	Finds viscosity for non-condensable He, given the temperature.
HAT28	Finds enthalpy for non-condensable N_2 given the temperature.
HENRY	Finds Henry's constant for N_2 and water. (This function is not used.)
HFPSAT	Finds the liquid saturation enthalpy given the pressure.
HGPSAT	Finds the vapor saturation enthalpy given the pressure.
SIGTF	Finds the surface tension of water.
TSATF	Given the pressure, this returns the saturation temperature.
VFT	Given the saturation temperature, this function finds the density of water.
VGPT	Finds specific volume given pressure and temperature.

Section 5

Input and Output

This section describes the input parameters necessary to run this computer code and an explanation of all the associated output.

INPUT

Table 5.1 defines all the input parameters. The inputs are divided into five basic groups, as follows:

1. Geometric parameters
2. Inlet conditions
3. Heat input
4. Pressure drop parameters
5. Integration and Printing parameters

Each input variable is on a separate line in the input file. The variables must be input in the following order.

Line 1: MN, MV, WIDE, HIGH, TUBEL, THETA
Line 2: TIN, PIN, VIN
Line 3: QW, ZHEATS, ZHEATF
Line 4: ELOSSIRR, ELOSSREV
Line 5: BETA
Line 6: ZPRNT

Table 5.1
Input Definition

1. Geometric Parameters

Parameter	Units	Description
HIGH	Meters	Height of channel cross section
WIDE	Meters	Width of channel cross-section
THETA	Degrees	Angle of orientation from horizontal
TUBEL	Meters	Channel length

2. Inlet Conditions

Parameter	Units	Description
BETA	1/Degre K	Liquid thermal expansion coefficient
MN	kg/kgmole	Molecular weight of noncondensibles
MV	kg/kgmole	Molecular weight of water vapor
PIN	Pa	Inlet pressure of fluid
TIN	°C	Inlet temperature of fluid
VIN	m/s	Inlet velocity of fluid

3. Heat Input

Parameter	Units	Description
QW	W/m	Heat input rate per unit of channel length
ZHEATS	M	Location along channel where heat input begins
ZHEATF	M	Location along channel where heat input ends

4. Pressure Drop Parameters

Parameter	Units	Description
ELOSSIRR	-	Irreversible Loss Coefficient at Inlet
ELOSSREV	-	Reversible Pressure drop Coefficient at Inlet

5. Integration and Printing Parameters

Parameter	Units	Description
ZPRNT	m	Printing Increment

Output Information

Includes:

1. All input variables
2. Local conditions along length of channel, divided by flow regimes. Pressure and enthalpy are given at all locations. At the locations where two phase flow occurs, the quality, x , and void fraction, α , are given as well as the gas and liquid velocities, u_g and u_f , respectively, where appropriate.
3. Location of onset of boiling, switch to film flow calculations and location of single-phase vapor flow are printed out.

Section 6

Sample Input and Output

Sample Input

29.0,18.0,0.005,0.06,0.21,0.0,
 20.0,2.03e6,0.3,
 1.5E6,.01,0.2,
 .3,.5,
 304.E-6,
 0.001

Sample Output

PROGRAM INPUT DATA

Molecular Weights of Noncondensibles and Water

MN = 29.0000 MV = 18.0000

Channel Width	Channel Height	Length	Angle of Inclination
.0050	.0600	.2100	.0000

Inlet Conditions

Temperature (Deg C)	Pressure (Pa)	Velocity (m/s)
20.000000	2030000.000000	.300000

Heat Input = .150000E+07 W/m

Heating starts at z = .010000 m

Heating ends at z = .200000 m

Inlet irreversible loss coefficient = .300

Inlet reversible loss coefficient = .500

Thermal expansion coef. of liquid = 3.04000E-04 1/K

Print interval = 1.00000E-03 m

Liquid Single Phase Results

z (m)	T (K)	P (Pa)	Xeq (--)
.00000	293.15	2.0300E+06	-3.0963E-01
.00100	321.95	2.0300E+06	-3.9534E-01
.00200	321.95	2.0300E+06	-3.9534E-01
.00300	321.95	2.0300E+06	-3.9534E-01

.00400	321.95	2.0300E+06	-3.9534E-01
.00500	321.95	2.0300E+06	-3.9534E-01
.00600	321.95	2.0300E+06	-3.9534E-01
.00700	321.95	2.0300E+06	-3.9534E-01
.00800	321.95	2.0300E+06	-3.9534E-01
.00900	321.95	2.0300E+06	-3.9534E-01
.01000	321.95	2.0300E+06	-3.9534E-01
.01100	325.62	2.0300E+06	-3.8651E-01
.01200	329.30	2.0300E+06	-3.7768E-01
.01300	332.98	2.0300E+06	-3.6885E-01
.01400	336.65	2.0300E+06	-3.6002E-01
.01500	340.33	2.0300E+06	-3.5119E-01
.01600	344.00	2.0300E+06	-3.4237E-01
.01700	347.68	2.0300E+06	-3.3354E-01
.01800	351.36	2.0300E+06	-3.2471E-01
.01900	355.03	2.0300E+06	-3.1588E-01
.02000	358.71	2.0300E+06	-3.0705E-01
.02100	362.38	2.0300E+06	-2.9822E-01
.02200	366.06	2.0300E+06	-2.8939E-01
.02300	369.74	2.0300E+06	-2.8056E-01
.02400	373.41	2.0300E+06	-2.7173E-01
.02500	377.09	2.0300E+06	-2.6290E-01
.02600	380.76	2.0300E+06	-2.5407E-01
.02700	384.44	2.0300E+06	-2.4524E-01
.02800	388.12	2.0300E+06	-2.3641E-01
.02900	391.79	2.0300E+06	-2.2758E-01
.03000	395.47	2.0300E+06	-2.1875E-01
.03100	399.14	2.0300E+06	-2.0993E-01
.03200	402.82	2.0300E+06	-2.0110E-01
.03300	406.50	2.0300E+06	-1.9227E-01
.03400	410.17	2.0300E+06	-1.8344E-01
.03500	413.85	2.0300E+06	-1.7461E-01
.03600	417.52	2.0300E+06	-1.6578E-01
.03700	421.20	2.0300E+06	-1.5695E-01
.03800	424.88	2.0300E+06	-1.4812E-01
.03900	428.55	2.0300E+06	-1.3929E-01
.04000	432.23	2.0300E+06	-1.3046E-01
.04100	435.90	2.0300E+06	-1.2163E-01
.04200	439.58	2.0300E+06	-1.1280E-01
.04300	443.26	2.0300E+06	-1.0397E-01
.04400	446.93	2.0300E+06	-9.5144E-02
.04500	450.61	2.0299E+06	-8.6314E-02
.04600	454.28	2.0299E+06	-7.7485E-02
.04700	457.96	2.0299E+06	-6.8655E-02
.04800	461.64	2.0299E+06	-5.9826E-02
.04900	465.31	2.0299E+06	-5.0997E-02

.05000	468.99	2.0299E+06	-4.2167E-02
.05100	472.66	2.0299E+06	-3.3338E-02
.05200	476.34	2.0299E+06	-2.4509E-02
.05300	480.02	2.0299E+06	-1.5679E-02
.05400	483.69	2.0299E+06	-6.8500E-03

** Boiling Started at z = .0550 (m)

Boiling Region Results

z (m)	P (Pa)	Xeq (--)	Void (--)	Ug (m/s)	Uf (m/s)
.05600	2.0299E+06	1.0923E-02	4.1272E-01	7.8134E-01	5.9404E-01
.05700	2.0298E+06	1.9814E-02	5.3857E-01	1.0880E+00	7.4931E-01
.05800	2.0298E+06	2.8621E-02	6.1971E-01	1.3707E+00	9.0098E-01
.05900	2.0297E+06	3.7630E-02	6.7914E-01	1.6387E+00	1.0582E+00
.06000	2.0297E+06	4.6165E-02	7.2427E-01	1.9004E+00	1.2200E+00
.06100	2.0296E+06	5.5174E-02	7.5843E-01	2.1623E+00	1.3796E+00
.06200	2.0296E+06	6.4183E-02	7.8357E-01	2.4292E+00	1.5255E+00
.06300	2.0296E+06	7.2704E-02	8.0019E-01	2.7081E+00	1.6368E+00
.06400	2.0295E+06	8.1729E-02	8.1164E-01	2.9946E+00	1.7198E+00
.06500	2.0295E+06	9.1415E-02	8.2191E-01	3.2778E+00	1.8015E+00
.06600	2.0295E+06	9.9835E-02	8.3116E-01	3.5584E+00	1.8817E+00
.06700	2.0294E+06	1.0909E-01	8.3952E-01	3.8369E+00	1.9603E+00
.06800	2.0294E+06	1.1834E-01	8.4711E-01	4.1137E+00	2.0372E+00
.06900	2.0294E+06	1.2574E-01	8.5403E-01	4.3890E+00	2.1124E+00
.07000	2.0293E+06	1.3499E-01	8.6036E-01	4.6630E+00	2.1859E+00
.07100	2.0293E+06	1.4424E-01	8.6617E-01	4.9360E+00	2.2576E+00
.07200	2.0292E+06	1.5259E-01	8.7153E-01	5.2082E+00	2.3275E+00
.07300	2.0292E+06	1.6375E-01	8.7648E-01	5.4795E+00	2.3956E+00
.07400	2.0292E+06	1.7212E-01	8.8108E-01	5.7501E+00	2.4619E+00
.07500	2.0291E+06	1.8050E-01	8.8535E-01	6.0201E+00	2.5265E+00
.07600	2.0291E+06	1.8887E-01	8.8933E-01	6.2896E+00	2.5893E+00
.07700	2.0290E+06	1.9724E-01	8.9306E-01	6.5586E+00	2.6503E+00
.07800	2.0290E+06	2.0561E-01	8.9655E-01	6.8271E+00	2.7096E+00
.07900	2.0290E+06	2.1678E-01	8.9982E-01	7.0953E+00	2.7671E+00
.08000	2.0289E+06	2.2515E-01	9.0291E-01	7.3631E+00	2.8229E+00
.08100	2.0289E+06	2.3359E-01	9.0581E-01	7.6306E+00	2.8769E+00
.08200	2.0288E+06	2.4203E-01	9.0856E-01	7.8978E+00	2.9291E+00
.08300	2.0288E+06	2.5047E-01	9.1115E-01	8.1647E+00	2.9796E+00
.08400	2.0287E+06	2.5891E-01	9.1361E-01	8.4314E+00	3.0283E+00
.08500	2.0287E+06	2.6735E-01	9.1594E-01	8.6979E+00	3.0752E+00
.08600	2.0287E+06	2.8001E-01	9.1815E-01	8.9642E+00	3.1203E+00
.08700	2.0286E+06	2.8845E-01	9.2026E-01	9.2303E+00	3.1636E+00
.08800	2.0286E+06	2.9689E-01	9.2226E-01	9.4963E+00	3.2051E+00
.08900	2.0285E+06	3.0532E-01	9.2417E-01	9.7621E+00	3.2447E+00
.09000	2.0285E+06	3.1376E-01	9.2599E-01	1.0028E+01	3.2824E+00
.09100	2.0284E+06	3.2220E-01	9.2773E-01	1.0293E+01	3.3183E+00

.09200	2.0284E+06	3.3064E-01	9.2939E-01	1.0559E+01	3.3523E+00
.09300	2.0283E+06	3.3908E-01	9.3098E-01	1.0824E+01	3.3843E+00
.09400	2.0282E+06	3.4971E-01	9.3250E-01	1.1089E+01	3.4144E+00
.09500	2.0282E+06	3.5612E-01	9.3396E-01	1.1355E+01	3.4425E+00
.09600	2.0281E+06	3.6895E-01	9.3535E-01	1.1620E+01	3.4686E+00
.09700	2.0281E+06	3.7536E-01	9.3669E-01	1.1885E+01	3.4927E+00
.09800	2.0280E+06	3.8819E-01	9.3797E-01	1.2150E+01	3.5146E+00
.09900	2.0280E+06	3.9460E-01	9.3920E-01	1.2415E+01	3.5345E+00
.10000	2.0279E+06	4.0101E-01	9.4038E-01	1.2680E+01	3.5522E+00
.10100	2.0279E+06	4.1384E-01	9.4151E-01	1.2946E+01	3.5677E+00
.10200	2.0278E+06	4.2025E-01	9.4260E-01	1.3211E+01	3.5809E+00
.10300	2.0277E+06	4.2666E-01	9.4364E-01	1.3476E+01	3.5919E+00
.10400	2.0277E+06	4.3948E-01	9.4464E-01	1.3741E+01	3.6005E+00
.10500	2.0276E+06	4.4589E-01	9.4560E-01	1.4006E+01	3.6067E+00
.10600	2.0275E+06	4.5872E-01	9.4652E-01	1.4272E+01	3.6105E+00
.10700	2.0275E+06	4.6513E-01	9.4740E-01	1.4537E+01	3.6118E+00
.10800	2.0274E+06	4.7154E-01	9.4825E-01	1.4803E+01	3.6106E+00
.10900	2.0273E+06	4.8437E-01	9.4906E-01	1.5068E+01	3.6067E+00
.11000	2.0273E+06	4.9078E-01	9.4983E-01	1.5334E+01	3.6002E+00

Switch to Film Flow at z = .1110(m)

Film Region Results

z (m)	P (Pa)	Xeq (--)	Void (--)	Ug (m/s)	Uf (m/s)
.11100	2.0271E+06	5.0601E-01	9.5223E-01	1.5894E+01	3.6368E+00
.11200	2.0271E+06	5.1484E-01	9.5386E-01	1.6171E+01	3.6991E+00
.11300	2.0270E+06	5.2366E-01	9.5527E-01	1.6449E+01	3.7547E+00
.11400	2.0269E+06	5.3249E-01	9.5731E-01	1.6727E+01	3.8380E+00
.11500	2.0269E+06	5.4132E-01	9.5904E-01	1.7005E+01	3.9114E+00
.11600	2.0268E+06	5.5014E-01	9.6008E-01	1.7282E+01	3.9571E+00
.11700	2.0268E+06	5.5897E-01	9.6205E-01	1.7560E+01	4.0466E+00
.11800	2.0267E+06	5.6780E-01	9.6298E-01	1.7838E+01	4.0904E+00
.11900	2.0266E+06	5.7662E-01	9.6390E-01	1.8116E+01	4.1343E+00
.12000	2.0265E+06	5.8545E-01	9.6514E-01	1.8394E+01	4.1953E+00
.12100	2.0265E+06	5.9427E-01	9.6694E-01	1.8671E+01	4.2870E+00
.12200	2.0264E+06	6.0310E-01	9.6788E-01	1.8949E+01	4.3369E+00
.12300	2.0263E+06	6.1192E-01	9.6881E-01	1.9227E+01	4.3869E+00
.12400	2.0263E+06	6.2075E-01	9.7060E-01	1.9505E+01	4.4869E+00
.12500	2.0262E+06	6.2958E-01	9.7147E-01	1.9783E+01	4.5369E+00
.12600	2.0261E+06	6.3840E-01	9.7231E-01	2.0061E+01	4.5869E+00
.12700	2.0260E+06	6.4723E-01	9.7395E-01	2.0339E+01	4.6868E+00
.12800	2.0260E+06	6.5605E-01	9.7475E-01	2.0617E+01	4.7368E+00
.12900	2.0259E+06	6.6488E-01	9.7552E-01	2.0895E+01	4.7868E+00
.13000	2.0258E+06	6.7370E-01	9.7675E-01	2.1173E+01	4.8676E+00
.13100	2.0257E+06	6.8253E-01	9.7756E-01	2.1451E+01	4.9228E+00

.13200	2.0256E+06	6.9135E-01	9.7835E-01	2.1730E+01	4.9780E+00
.13300	2.0256E+06	7.0017E-01	9.7934E-01	2.2008E+01	5.0482E+00
.13400	2.0255E+06	7.0900E-01	9.7982E-01	2.2286E+01	5.0833E+00
.13500	2.0254E+06	7.1782E-01	9.8076E-01	2.2564E+01	5.1535E+00
.13600	2.0253E+06	7.2665E-01	9.8168E-01	2.2842E+01	5.2237E+00
.13700	2.0252E+06	7.3547E-01	9.8258E-01	2.3121E+01	5.2939E+00
.13800	2.0251E+06	7.4430E-01	9.8345E-01	2.3399E+01	5.3641E+00
.13900	2.0250E+06	7.5312E-01	9.8387E-01	2.3677E+01	5.3992E+00
.14000	2.0250E+06	7.6194E-01	9.8471E-01	2.3956E+01	5.4694E+00
.14100	2.0249E+06	7.7077E-01	9.8553E-01	2.4234E+01	5.5396E+00
.14200	2.0248E+06	7.7959E-01	9.8632E-01	2.4512E+01	5.6098E+00
.14300	2.0247E+06	7.8841E-01	9.8710E-01	2.4791E+01	5.6801E+00
.14400	2.0246E+06	7.9724E-01	9.8748E-01	2.5069E+01	5.7152E+00
.14500	2.0245E+06	8.0606E-01	9.8823E-01	2.5348E+01	5.7854E+00
.14600	2.0244E+06	8.1488E-01	9.8896E-01	2.5626E+01	5.8556E+00
.14700	2.0243E+06	8.2371E-01	9.8967E-01	2.5905E+01	5.9259E+00
.14800	2.0242E+06	8.3253E-01	9.9037E-01	2.6184E+01	5.9961E+00
.14900	2.0241E+06	8.4135E-01	9.9105E-01	2.6462E+01	6.0664E+00
.15000	2.0240E+06	8.5017E-01	9.9138E-01	2.6741E+01	6.1015E+00
.15100	2.0239E+06	8.5900E-01	9.9204E-01	2.7020E+01	6.1718E+00
.15200	2.0238E+06	8.6782E-01	9.9268E-01	2.7298E+01	6.2420E+00
.15300	2.0237E+06	8.7664E-01	9.9331E-01	2.7577E+01	6.3123E+00
.15400	2.0236E+06	8.8546E-01	9.9392E-01	2.7856E+01	6.3826E+00
.15500	2.0235E+06	8.9428E-01	9.9423E-01	2.8135E+01	6.4177E+00
.15600	2.0234E+06	9.0311E-01	9.9482E-01	2.8414E+01	6.4880E+00
.15700	2.0233E+06	9.1193E-01	9.9540E-01	2.8692E+01	6.5583E+00
.15800	2.0232E+06	9.2075E-01	9.9597E-01	2.8971E+01	6.6286E+00
.15900	2.0231E+06	9.2957E-01	9.9653E-01	2.9250E+01	6.6989E+00
.16000	2.0230E+06	9.3839E-01	9.9680E-01	2.9529E+01	6.7341E+00
.16100	2.0229E+06	9.4721E-01	9.9734E-01	2.9808E+01	6.8044E+00
.16200	2.0227E+06	9.5603E-01	9.9787E-01	3.0087E+01	6.8747E+00
.16300	2.0226E+06	9.6485E-01	9.9839E-01	3.0366E+01	6.9450E+00
.16400	2.0225E+06	9.7367E-01	9.9890E-01	3.0646E+01	7.0153E+00
.16500	2.0224E+06	9.8249E-01	9.9915E-01	3.0925E+01	7.0505E+00
.16600	2.0223E+06	9.9131E-01	9.9964E-01	3.1204E+01	7.1208E+00

Complete Evaporation at $z = .1670(\text{m})$

Superheated Single Phase Results

z (m)	T (K)	P (Pa)	H (J/kg) (--)
.16800	495.75	2.0220E+06	2.8147E+06
.16900	505.06	2.0218E+06	2.8313E+06
.17000	514.33	2.0216E+06	2.8480E+06

.17100	523.58	2.0214E+06	2.8647E+06
.17200	530.76	2.0212E+06	2.8813E+06
.17300	540.73	2.0211E+06	2.8980E+06
.17400	550.62	2.0209E+06	2.9146E+06
.17500	567.63	2.0207E+06	2.9313E+06
.17600	567.63	2.0205E+06	2.9479E+06
.17700	573.42	2.0203E+06	2.9646E+06
.17800	580.50	2.0201E+06	2.9813E+06
.17900	588.76	2.0200E+06	2.9979E+06
.18000	597.82	2.0198E+06	3.0146E+06
.18100	610.65	2.0196E+06	3.0312E+06
.18200	623.43	2.0194E+06	3.0479E+06
.18300	623.43	2.0192E+06	3.0645E+06
.18400	629.81	2.0190E+06	3.0812E+06
.18500	639.49	2.0189E+06	3.0979E+06
.18600	646.33	2.0187E+06	3.1145E+06
.18700	659.97	2.0185E+06	3.1312E+06
.18800	666.76	2.0183E+06	3.1478E+06
.18900	673.54	2.0181E+06	3.1645E+06
.19000	677.86	2.0179E+06	3.1812E+06
.19100	686.94	2.0178E+06	3.1978E+06
.19200	696.50	2.0176E+06	3.2145E+06
.19300	703.30	2.0174E+06	3.2311E+06
.19400	710.09	2.0172E+06	3.2478E+06
.19500	723.63	2.0170E+06	3.2644E+06
.19600	726.46	2.0169E+06	3.2811E+06
.19700	735.64	2.0167E+06	3.2978E+06
.19800	748.35	2.0165E+06	3.3144E+06
.19900	755.10	2.0163E+06	3.3311E+06
.20000	764.57	2.0161E+06	3.3477E+06
.20100	764.57	2.0161E+06	3.3477E+06
.20200	764.57	2.0161E+06	3.3477E+06
.20300	764.57	2.0161E+06	3.3477E+06
.20400	764.57	2.0161E+06	3.3477E+06
.20500	764.57	2.0160E+06	3.3477E+06
.20600	764.57	2.0160E+06	3.3477E+06
.20700	764.57	2.0160E+06	3.3477E+06
.20800	764.57	2.0160E+06	3.3477E+06
.20900	764.57	2.0160E+06	3.3477E+06
.21000	764.57	2.0160E+06	3.3477E+06

PEXIT= .201E+07

Appendix B

DROPCON: A Computer Program for Condensate Droplet Growth in a Vapor- Noncondensable Mixture Undergoing Depressurization

Authors:
Jinhua Yan
S. M. Ghiaasiaan

Submitted by:
G.W. Woodruff School of Mechanical Engineering
Georgia Institute of Technology
Atlanta, GA 30332-0405

Submitted to:

Tyndall Air Force Base
FL 32403-5526

January 18, 2002

Table of Contents

Section	Page
Table of Contents	2
1. Introduction	3
1.1 Problem Background	3
1.2 Report Summary	3
2. Description of Theory	4
3. Code Structure	
4. Description of Subroutines and Functions	7
5. Input and Output	8
6. Sample Runs	11
7. Reference	15

Section 1

Introduction

1.1 Problem Background

DROPCON is a computer code that has been developed to model the condensation and condensate droplet growth phenomena resulting from the depressurization of a vapor-noncondensable mixture. The code is meant to be a generic analytical tool for the calculation of exit conditions of components such as turbine expanders.

The code assumes that a known flow rate of a vapor-noncondensable mixture, initially at saturation conditions, flows into a device that imposes a pressure drop to the flow field. The conditions of the flow mixture at the exit of the device are then calculated by the code. Parameters that are calculated are meant to be sufficient for modeling the droplet removal phenomena in a separator/dryer component.

1.2 Report Summary

Section 2 briefly describes the phenomena that are modeled in this computer code. The code structure along with its flow diagram is presented in Section 3. Section 4 briefly describes each of the routines used in the code. The input and output are described in Section 5. A sample case is provided in Section 6, where a complete listing of all the input and output is included. The references are listed in Section 7.

Section 2

Description of Theory

A schematic diagram of the modeled system is shown in Figure 1. The system is basically a control volume with an arbitrary configuration. Furthermore, it is assumed to exchange mechanical work with its surroundings. At Port 1, the inlet port, a known flow rate of a saturated mixture of a vapor (steam at this time) and a non-condensable (air at this time) with known thermodynamic conditions (pressure, vapor mass fraction) is mixed with a known flow rate of saturated droplets sprayed into the flow field. The mixture is then assumed to undergo depressurization, and leave the systems at Port 2, the exit port, while it has reached at thermodynamic equilibrium. It is also assumed that the pressure drop in the system is known.

The model is based on the following assumptions.

1. Thermodynamic equilibrium is maintained throughout the system.
2. Liquid is impermeable to the non-condensable.
3. The non-condensable is an ideal gas.
4. Excluding the inlet and outlet ports, no mass transfer takes place anywhere else between the modeled system and the surroundings.
5. The liquid-gas mixture is homogeneous at both inlet and exit ports.
6. If droplets are injected into the stream at inlet, the injected spray droplets at inlet have a log-normal size distribution with known distribution characteristics.

Consistent with the above assumptions, the conservation equations for the total mass, the condensable (liquid + vapor) mass, and total energy (thermal and mechanical) are iteratively solved, thereby the exit thermodynamic conditions, as well as the mass flow rates of vapor, non-condensable and droplets, are calculated.

Four different types of expanders are modeled. The following table is a summary of the properties of the modeled expander types.

Expander Type	Description
1	Inlet and outlet pressures are known; droplets with known size distribution are injected at inlet.
2	Turbine with known Input pressure, output power, and isentropic efficiency; fog formation takes place.
3	Turbine with known Input pressure, output power, and isentropic efficiency; droplets with known size distribution are injected at inlet.
4	Inlet and outlet pressures are known; fog formation takes place.

The injected droplets, when applicable, are assumed log-normally distributed with respect to their diameters. The droplets leaving the system are also assumed to have a log-normal size distribution, with a geometric standard deviation equal to that at the inlet. This is equivalent to the assumption that the shape of the size distribution does not change, and only the distribution curve moves towards a larger size. The code thus calculates the size distribution characteristics of the droplets at the exit.

At present the code is equipped with property routine for water/steam (the condensate) and air (the non-condensable).

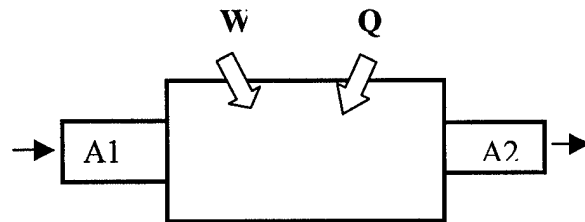


Figure 1

Schematic of the Modeled System

Section 4

Description of Subroutines and Functions

This section contains a description of subroutines and functions used in this computer code.

Subroutines:

TURV1	Models the first type of turbine expander.
FS1	Calculates the function values for the first type turbine.
TURV2	Models the second type of turbine expander.
FS2	Calculates the function values for the second type turbine.
TURV3	Models the third type of turbine expander.
COE	Calculates the coefficients of each equation at each iteration for the FS1,FS2 and FS3 subroutines.
FS3	Calculates the function values for the third type turbine.
TURV4	Models the fourth type of turbine expander.
FS4	Calculates the function values for the fourth type turbine.
PNEWTON	Solves the set of non-linear equations.
AGAUS	Solves the set of linear equations.
POLINT	This is a Lagrangian interpolation routine, is used to interpolate between thermodynamic values in property tables.

Functions:

TSATF

Given the pressure, this returns the saturation temperature. T in K, P in bar.

VFT

Given the saturation temperature, this finds the density of water. T in K, density in kg/m^3 .

HFPSAT

Finds the liquid saturation enthalpy given the pressure. P in bar, enthalpy in J/kg.

HGPSAT

Finds the vapor saturation enthalpy given the pressure. P in bar, enthalpy in J/kg.

HAT29

Finds enthalpy for non-condensable AIR given the temperature. T in K, enthalpy in kJ/kg.

VGPT

Finds specific volume given pressure and temperature, P in bar, T in K, and VG in cm^3/g .

SAT29

Finds entropy of non-condensable AIR given the temperature. T in K and SAT29 in J/kg.K.

SGPSAT

Finds entropy of saturated vapor in partial pressure of vapor given the temperature. T in C, and entropy in J/kg.K

SFPSAT

Finds entropy of saturated liquid (water) in vapor partial pressure given the temperature. T in C, and entropy in J/kg.K

Section 5

Input and output

This section describes the input parameters necessary to run this computer code and an explanation of all the associated output.

INPUT:

Table 2 defines all the input parameters for TURV1, the first expander type. For other expander types the definition of parameters are the same. The sample input data files, to be given shortly, provide the exact order of input parameter that should be provided.

Table 2

Parameters	units	Description
W	J	Turbine power
P1	bar	Inlet pressure
P2	bar	Outlet pressure
MF1	kg/s	Mass flow rate of liquid at inlet
E1		Volume fraction occupied by liquid
NT1	m ⁻³	Total number density of droplets at inlet
SIG		Geometric standard deviation
R	m ³ .bar/(kmol.K)	Universal gas constant
MN	kg/kmole	Molar mass of non-condensable
MV	kg/kmole	Molar mass of water
U1	m/s	Mixture velocity at inlet
A2	m ²	Outlet area
MG1	kg/s	Mass flow rate of gas mixture at inlet
MV1	kg/s	Mass flow rate of vapor at inlet
MN1	kg/s	Mass flow rate of non-condensable at inlet
PREF	bar	Reference pressure for entropy
TREF	K	Reference temperature for entropy

OUTPUT:

Two different types of output are generated by the code. One type of output file, with the generic name TURVn.out, where n represents the expander type, provides detailed and well-defined information regarding the exit conditions of the expander. Another output file with generic name CYC-n.dat, with n representing the expander type, is also generated. This file can be used as the input file for the code CYCSEP which models a cyclone-type separator. Only the parameters in the former data files are described below.

Table 3 defines all output parameters for TURV1.out, TURV2.out, TURV3.out, and TURV4.out. (They are all formatted the same way.)

Table 3

Parameters	Units	Description
U2	m/s	Outlet velocity of gas mixture
A2	m ²	Outlet area
W	J	turbine power
E2		Volume fraction occupied by liquid
XN2		Mass fraction of noncondensable in gas mixture
YN2		Mole fraction of noncondensable in gas mixture
PV2	bar	Partial pressure of vapor in gas mixture
PN2	bar	Partial pressure of noncondensable in gas mixture
T2	K	Temperature of gas mixture
HG2	J/kg	Enthalpy of gas mixture
RHOG2	kg/m ³	Density of gas mixture
SIG		Geometric standard deviation
INCMD		Log median diameter
DV	m	Volume-averaged droplet diameter

Section 6

Sample Input and Output

6.1.1 Sample Input For the First Expander Type

0.0, 5.5, 1.5, 0.02,
1.e-6, 1.e08, 2.0, 0.0831434, 29.0, 18.0, 2.0, 2.02683E-3,
0.08, 0.04, 0.04,
1.0, 100.0

6.1.2 Sample Output For the First Expander Type

OUTLET:

U2= .362170D+02

A2= .202683D-02

W= .000000D+00

E2= .286907D-03

XN2= .501698D+00

YN2= .384585D+00

PV2= .923123D+00

PN2= .576877D+00

T2= .370557D+03

HG2= .151829D+07

RHOG2= .108646D+01

GEOMETRIC STANDARD DEVIATION IS .200000D+01

LOG MEDIAN DIAMETER IS: -.100847D+02

MEDIAN OF VOLUME DISTRIBUTION IS: .176298D-03

6.2.1 Sample Input For the Second Expander Type

5696.46,5.5, 1.3,
1.e-6,1.e08,2.0,0.0831434,29.0,18.0,2.0,2.02683E-3,
0.08,0.04,0.04,
1.0,100.0

6.2.2 Sample Input For the Second Expander Type

OUTLET:

U2= .405622D+02

A2= .202683D-02

W= .569646D+04

E2= .184247D-04

XN2= .509310D+00

YN2= .391817D+00

PV2= .790637D+00

PN2= .509363D+00

T2= .366344D+03

HG2= .149590D+07

RHOG2= .955316D+00

SG2= .349689D+04

SF2= .219397D+04

GEOMETRIC STANDARD DEVIATION IS .200000D+01

LOG MEDIAN DIAMETER IS: -.109998D+02

MEDIAN OF VOLUME DISTRIBUTION IS: .705994D-04

6.3.1 Sample Input For the Third Expander Type

3580.12,5.5, 1.3,0.02,
1.e-6,1.e08,2.0,0.0831434,29.0,18.0,2.0,2.02683E-3,
0.08,0.04,0.04,
1.0,100.0

6.3.2 Sample Input For the Third Expander Type

OUTLET:

U2= .406802D+02

A2= .202683D-02

W= .358012D+04

E2= .161475D-04

XN2= .508165D+00

YN2= .390726D+00

PV2= .792057D+00

PN2= .507943D+00

T2= .366392D+03

HG2= .149859D+07

RHOG2= .954689D+00

SG2= .349666D+04

SF2= .219397D+04

GEOMETRIC STANDARD DEVIATION IS .200000D+01

LOG MEDIAN DIAMETER IS: -.110438D+02

MEDIAN OF VOLUME DISTRIBUTION IS: .675620D-04

6.4.1 Sample Input For the Fourth Expander Type

0.0,5.5, 2.5,
1.e-6,1.e08,2.0,0.0831434,29.0,18.0,2.0,2.02683E-3,
0.08,0.04,0.04,
1.0,100.0

6.4.2 Sample Input For the Fourth Expander Type

OUTLET:

U2= .225896D+02

A2= .202683D-02

W= .000000D+00

E2= .299214D-05

XN2= .500816D+00

YN2= .383750D+00

PV2= .154062D+01

PN2= .959376D+00

T2= .385332D+03

HG2= .152803D+07

RHOG2= .174445D+01

GEOMETRIC STANDARD DEVIATION IS .200000D+01

LOG MEDIAN DIAMETER IS: -.116057D+02

MEDIAN OF VOLUME DISTRIBUTION IS: .385178D-04

Appendix C

User's Manual for Cyclone Code CYCSEP

Authors:

Jinhua Yan
S. M. Ghiaasiaan

Submitted by:

G.W.Woodruff School of Mechanical Engineering
Georgia Institute of Technology
Atlanta, GA 30332-0405

Submitted to:

Tyndall Air Force Base
FL 32403-5526

January 18, 2002

Table of Contents

Section	Page
Table of Contents	2
1. Introduction	3
1.1 Problem Background	3
1.2 Report Summary	3
2. Description of Subroutines and Functions	5
3. Input and Output	7
4. Sample input and output	10
5. References	14

Section 1

1. Introduction

1.1 Problem Background

CYCSEP is a computer code that has been developed to model the condensation and droplet removal in a system consisting of a cyclone-type separator. Condensation takes place as a result of the depressurization of a vapor-noncondensable mixture, while droplet removal is caused by the impaction of droplets with the cyclone walls.

CYCSEP should be used in tandem with the computer code DROPCON, and uses two input files. One input file, named CYCGMTRY.DAT, contains geometrical parameters for the cyclone separator. In addition, CYCSEP uses an output file directly generated by the DRPCOND code package. Therefore, before CYCSEP is used, DROPCON must be run, so that the aforementioned input data file for CYCSEP is automatically generated. Thus, a review of the user's manual for DROPCON is necessary before the present code is used.

Figure 1 is a schematic of the modeled separator. The separator model is a modification of a classical and widely-applied model (Leith and Licht, 1972). The latter model, in its original form, applies to the Figure 1(a). The modified model, however, is meant to represent an experimental test section displayed in Figure 1(b), and currently under development at Georgia Tech.

1.2 Report Summary

The phenomena that are modeled in this computer code package are described in Ghiaasiaan et al (2002) and will not be repeated here. Section 2 briefly describes each of the routines used in the code package. The input and output are described in Section 3. A sample case is provided in Section 4, where a complete listing of all the output is included. The references are listed in Section 5.

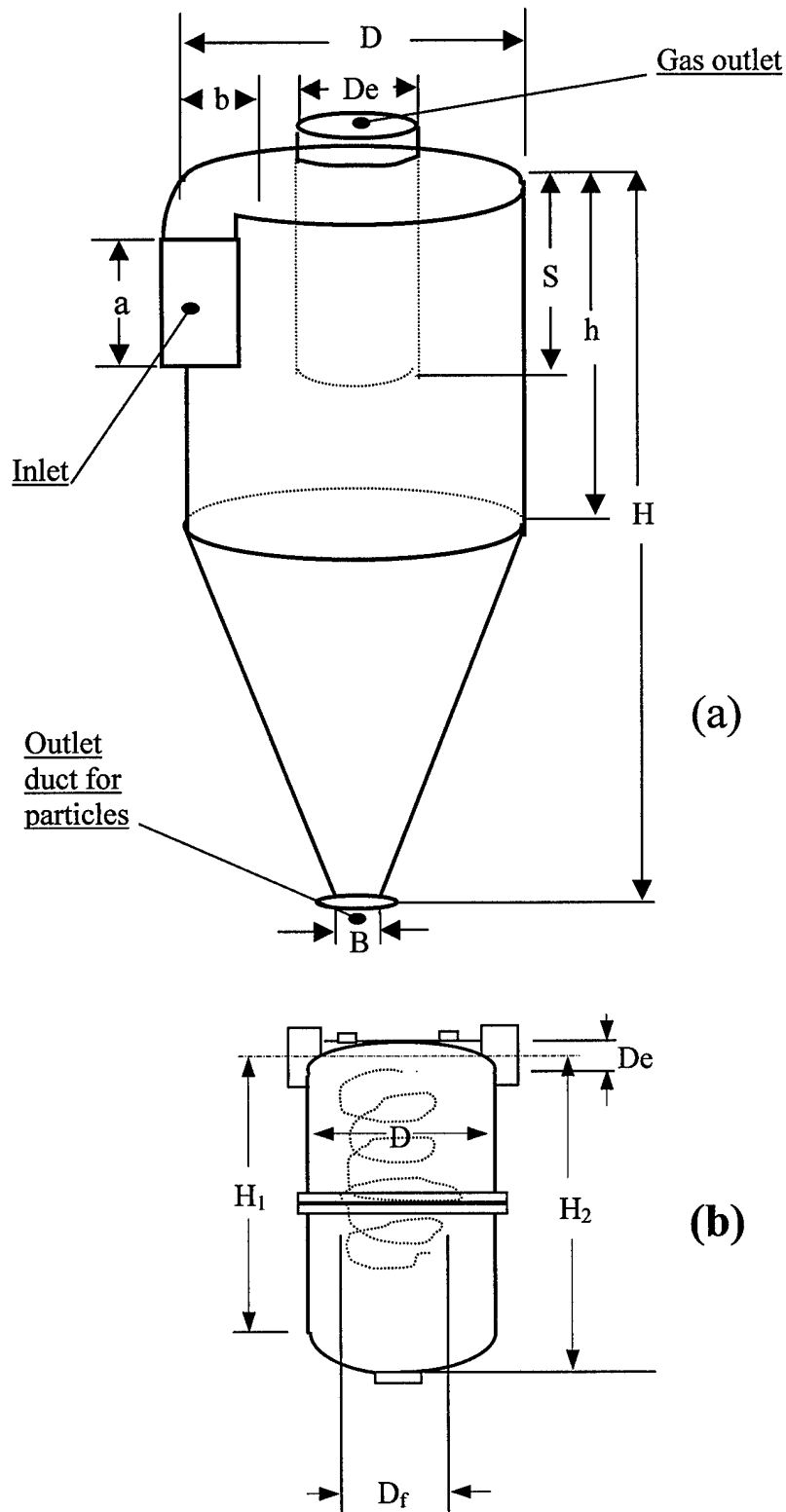


Fig. 1 Schematic of a Cyclone with Tangential Gas Inlet: (a) the system modeled by Leith and Licht, (1972); (b) the Georgia Tech test section

Section 2

Description of Subroutines and Functions

This section contains a description of each subroutine and function in this computer code. The reader is reminded that this code is meant to use the output provided by the code package DROPCON. The latter code package contains models for four different expanders. The expander types referred to in the forthcoming list are briefly described in the DROPCON manual, and in Ghiaasiaan et al. (2002). These documents should be consulted before the present code is applied.

Subroutines:

CYC1	Calculates the cyclone results when the cyclone is attached to the first turbine type.
CYC2	Calculates the cyclone results when the cyclone is attached to the second turbine type.
CYC3	Calculates the cyclone results when the cyclone is attached to the third turbine type.
CYC4	Calculates the cyclone results when the cyclone is attached to the fourth turbine type.
COE	Calculates the coefficients of each equation to be solved at each iteration.
FS	Calculates the numerical value of each equation using the results of COE.
PNEWTON	Solves the set of non-linear equations using Newton's method.
AGAUS	Solves the set of linear equations.
POLINT	This is a Lagrangian interpolation routine, and is used to interpolate between thermodynamic values in property tables.
VISCOV	Gets vapor viscosity EMU at given pressure P and temperature T, P in bar, T in K, EMU in Pa.s.

Functions:

TSATF	Given the pressure, this returns the saturation temperature. T in K, P in bar.
--------------	--

VFT

Given the saturation temperature, this finds the density of water. T in K, density in kg/m^3 .

HFPSAT

Finds the liquid saturation enthalpy given the pressure. P in bar, enthalpy in J/kg.

HGPSAT

Finds the vapor saturation enthalpy given the pressure. P in bar, enthalpy in J/kg.

HAT29

Finds enthalpy for non-condensable AIR given the temperature. T in K, enthalpy in kJ/kg.

VGPT

Finds specific volume given pressure and temperature, P in bar, T in K, and VG in cm^3/g .

Section 3

Input and output

This section describes the input parameters necessary to run this computer code, and provides an explanation of all the associated output.

INPUT

The input files for this code, as mentioned earlier, include two separate files. One input file, named CYCGMTRY.DAT, contains geometric parameters and outlet pressure. In addition another input file is automatically generated by the code package DRPCOND. Since the code uses input provided by four different expanders, the user must first specify the expander type. (For expander types, see the User's Manual for DROPCON Code).

Two different types of output files are generated by the DROPCON code. One type of output file, with the generic name TURVn.out, where n represents the expander type, provides detailed and well-defined information regarding the exit conditions of the expander. Another output file with generic name CYC-n.dat, with n representing the expander type, is also generated by DROPCON. This file is meant to be used as one of the input files for the code CYCSEP code.

The specification of the expander type by the user is done interactively. The CYCSEP code, once executed, enquires on the screen:

"Please enter the expander type (1-4)?"

In response, the user must type the expander type number, followed by a return. The code then does the following. If expander type 1 is specified by the user, the code searches for CYC-1.dat, and reads it. In case expander type is 2, then the code searches for CYC-2.dat, and so on.

Transfer of information from DROPCON to CYCSEP is thus automatic, as long as the correct expander type is specified by the user. A list of parameters provided by CYC-n.dat files will therefore not be provided here.

Table 1 is the list of parameters that are provided in the CYCGMTRY.DAT data file. Numerical values of these parameters must be typed into the file CYCGMTRY.DAT, in the same order as they appear in the table, with numbers separated from each other by a comma.

Table 2 is a list of the parameters that appear in the output from CYCSEP execution.

Table 1
List of Parameters Provided in CYCGMTRY.DAT

Parameters	units	Description
D	m	Body diameter of cyclone
DE	m	Pipe diameter at inlet and outlet
DF	ft	Diameter of cyclone body
H1	m	Height of cylindrical body
H2	m	Total cyclone height
VS	m ³	Annular-shaped volume above exit duct to mid level of entrance duct
MN	kg/kmole	Molar mass of noncondensable
MV	kg/kmole	Molar mass of water vapor
P2	bar	Mixture pressure at outlet
SIG		Geometric standard deviation

Table 2
List of Parameters in the Output Files

Parameters	Units	Description
A2	m ²	Area of outlet
U2	m/s	Velocity of mixture
E2		Volume fraction occupied by liquid
XN2		Mass fraction of noncondensable in gas mixture
YN2		Mole fraction of noncondensable in gas mixture
PV2	bar	Partial pressure of vapor in gas mixture
PN2	bar	Partial pressure of noncondensable in gas mixture
T2	K	Temperature of gas mixture
RHOF2	kg/m ³	Density of droplets
RHOG2	kg/m ³	Density of gas mixture
HG2	J/kg	Enthalpy of gas mixture
HF2	J/kg	Enthalpy of droplets
EMUG2	Pa.S	Viscosity of gas mixture
SIG		Geometric standard deviation
INCMD		Log mean diameter
DV2	m	droplets volumetric meandiameter
NT2	#/m ³	Total number density of droplets at outlet
ETA		Droplet removal efficiency

Section 4

Sample Input and Output

Sample input and output files for all options are provided in this section. Note that the input file CYCGMTRY.DAT is common for all of the options. Also, note that files with generic name cyc-n.dat are generated by the DROPCON computer code.

4.1.1 Sample CYCGMTRY.DAT Input File

0.168275, 5.08E-002, 0.1008, 0.4318, 0.53848, 1.3E-003
29.0, 18.0, 1.0, 2.0

4.1.2 Sample Input cyc-1.dat

0.0000000000000000E+000 2.026829769984279E-003 36.216971074700500
2.869072660026386E-004 5.016977999359462E-001 3.845848011661990E-001
9.231227982507015E-001 5.768772017492985E-001 370.557208463130800
1.0000000000000000E+008 1.762981513684647E-004
1518290.4266541230000000
1.086458155699219

4.1.3 Sample Output cyc-1.out

THE FOLLOWING IS THE CYCLONE RESULT FROM THE TURBINE
FIRST TYPE, W=0 MF1>0, OUTPUT DATA

OUTLET:

A2= .202683D-02

U2= .535646D+02

E2= .375018D-18

XN2= .494655D+00

YN2= .377939D+00

PV2= .622061D+00

PN2= .377939D+00

T2= .360030D+03

RHOF2= .969690D+03

RHOG2= .742217D+00

HG2= .152085D+07

HF2= .368708D+06

EMUG2= .152999D-04

GEOMETRIC STANDARD DEVIATION IS .200000D+01

LOG MEDIAN DIAMETER IS: -.101011D+02

MEDIAN OF VOLUME DISTRIBUTION IS: .173435D-03

TOTAL DROPLET NUMBER AT OUTLET IS: .144329D-06

REMOVAL EFFICIENCY ETA IS: .100000D+01

4.2.1 Sample Input cyc-2.dat

```
5696.456450794689000 2.026829769984279E-003 40.562175665823850
1.842470350576125E-005 5.093101708643396E-001 3.918174398295731E-001
7.906372992211506E-001 5.093626530951335E-001 366.343828883619500
1.000000000000000E+008 7.059935695044410E-005 1495899.0154097900000000
9.553161467587280E-001
```

4.2.2 Sample Output cyc-2.out

THE FOLLOWING IS THE CYCLONE RESULT FROM THE TURBINE
SECOND TYPE, W>0 MFL=0, OUTPUT DATA

OUTLET:

A2= .202683D-02

U2= .520967D+02

E2= .118021D-12

XN2= .505579D+00

YN2= .388266D+00

PV2= .611734D+00

PN2= .388266D+00

T2= .359598D+03

RHOF2= .969973D+03

RHOG2= .746845D+00

HG2= .149514D+07

HF2= .366588D+06

EMUG2= .153796D-04

GEOMETRIC STANDARD DEVIATION IS .200000D+01

LOG MEDIAN DIAMETER IS: -.110841D+02

MEDIAN OF VOLUME DISTRIBUTION IS: .648970D-04

TOTAL DROPLET NUMBER AT OUTLET IS: .108665D+01

REMOVAL EFFICIENCY ETA IS: .100000D+01

4.3.1 Sample Input cyc-3.dat

5114.459519643379000 2.026829769984279E-003 40.680241677380760
1.614753308588079E-005 5.081645586989505E-001 3.907256674766556E-001
7.920566032278834E-001 5.079433490884006E-001 366.391954182002000
1.000000000000000E+008 6.756202174997793E-005 1498594.811873642000000
9.546887900095444E-001

4.3.2 Sample Output cyc-3.out

THE FOLLOWING IS THE CYCLONE RESULT FROM THE TURBINE
THIRD TYPE, W>0 MFL>0, OUTP UT DATA

OUTLET:

A2= .202683D-02

U2= .522460D+02

E2= .184953D-12

XN2= .504451D+00

YN2= .387195D+00

PV2= .612805D+00

PN2= .387195D+00

T2= .359643D+03

RHOF2= .969944D+03

RHOG2= .746364D+00

HG2= .149779D+07

HF2= .366810D+06

EMUG2= .153713D-04

GEOMETRIC STANDARD DEVIATION IS .200000D+01

LOG MEDIAN DIAMETER IS: -.111406D+02

MEDIAN OF VOLUME DISTRIBUTION IS: .613306D-04

TOTAL DROPLET NUMBER AT OUTLET IS: .210937D+01

REMOVAL EFFICIENCY ETA IS: .100000D+01

4.4.1 Sample Input cyc-4.dat

0.000000000000000E+000 2.026829769984279E-003 22.589572022357500
2.992143576350699E-006 5.008160082856482E-001 3.837503288114426E-001
1.540624177971394 9.593758220286065E-001 385.331703469266300
1.000000000000000E+008 3.851779218993663E-005 1528026.628694685000000
1.744447088390374

4.4.2 Sample Output cyc-4.out

THE FOLLOWING IS THE CYCLONE RESULT FROM THE
TURBINE FOURTH TYPE, W=0 MFL=0, O

UTPUT DATA

OUTLET:

A2= .202683D-02

U2= .535646D+02

E2= .000000D+00

XN2= .494655D+00

YN2= .377939D+00

PV2= .622061D+00

PN2= .377939D+00

T2= .360030D+03

RHOF2= .969690D+03

RHOG2= .742217D+00

HG2= .152085D+07

HF2= .368708D+06

EMUG2= .152999D-04

GEOMETRIC STANDARD DEVIATION IS .200000D+01

LOG MEDIAN DIAMETER IS: -.107778D+02

MEDIAN OF VOLUME DISTRIBUTION IS: .881491D-04

TOTAL DROPLET NUMBER AT OUTLET IS: .144329D-06

REMOVAL EFFICIENCY ETA IS: .100000D+01

Section 5

References

Leith, D., and Licht, W., "The Collection Efficiency of Cyclone Type Particle Collectors – A New Theoretical Approach," AIChE Symp. Ser. 68, No. 126, pp. 196-206 (1972).

Ghiaasiaan, S.M., Yan, J., and McCord, B.B., "Numerical Models for Condenser and Evaporator Components of Fuel Cycles," Draft Final Report, Georgia Institute of Technology, January 2002.